

Role of Type I Interferon Signaling in Human Metapneumovirus Pathogenesis and Control of Viral Replication

Andrew K. Hastings,^a John J. Erickson,^a Jennifer E. Schuster,^c Kelli L. Boyd,^a Sharon J. Tollefson,^b Monika Johnson,^b Pavlo Gilchuk,^a Sebastian Joyce,^a  John V. Williams,^{a,b}

Departments of Pathology, Microbiology & Immunology^a and Pediatrics, Vanderbilt University School of Medicine, Nashville, Tennessee, USA^b; Department of Pediatrics, Children's Mercy Hospital, Kansas City, Missouri, USA^c

ABSTRACT

Type I IFN signaling, which is initiated through activation of the alpha interferon receptor (IFNAR), regulates the expression of proteins that are crucial contributors to immune responses. Paramyxoviruses, including human metapneumovirus (HMPV), have evolved mechanisms to inhibit IFNAR signaling, but the specific contribution of IFNAR signaling to the control of HMPV replication, pathogenesis, and adaptive immunity is unknown. We used IFNAR-deficient (IFNAR^{-/-}) mice to assess the effect of IFNAR signaling on HMPV replication and the CD8⁺ T cell response. HMPV-infected IFNAR^{-/-} mice had a higher peak of early viral replication but cleared the virus with kinetics similar to those of wild-type (WT) mice. However, IFNAR^{-/-} mice infected with HMPV displayed less airway dysfunction and lung inflammation. CD8⁺ T cells of IFNAR^{-/-} mice after HMPV infection expressed levels of the inhibitory receptor programmed death 1 (PD-1) similar to those of WT mice. However, despite lower expression of inhibitory programmed death ligand 1 (PD-L1), HMPV-specific CD8⁺ T cells of IFNAR^{-/-} mice were more functionally impaired than those of WT mice and upregulated the inhibitory receptor Tim-3. Analysis of the antigen-presenting cell subsets in the lungs revealed that the expansion of PD-L1^{low} dendritic cells (DCs), but not PD-L1^{high} alveolar macrophages, was dependent on IFNAR signaling. Collectively, our results indicate a role for IFNAR signaling in the early control of HMPV replication, disease progression, and the development of an optimal adaptive immune response. Moreover, our findings suggest an IFNAR-independent mechanism of lung CD8⁺ T cell impairment.

IMPORTANCE

Human metapneumovirus (HMPV) is a leading cause of acute respiratory illness. CD8⁺ T cells are critical for clearing viral infection, yet recent evidence shows that HMPV and other respiratory viruses induce CD8⁺ T cell impairment via PD-1–PD-L1 signaling. We sought to understand the role of type I interferon (IFN) in the innate and adaptive immune responses to HMPV by using a mouse model lacking IFN signaling. Although HMPV titers were higher in the absence of type I IFN, virus was nonetheless cleared and mice were less ill, indicating that type I IFN is not required to resolve HMPV infection but contributes to pathogenesis. Further, despite lower levels of the inhibitory ligand PD-L1 in mice lacking type I IFN, CD8⁺ T cells were more impaired in these mice than in WT mice. Our data suggest that specific antigen-presenting cell subsets and the inhibitory receptor Tim-3 may contribute to CD8⁺ T cell impairment.

Human metapneumovirus (HMPV) is a leading cause of acute lower respiratory infection (LRI), with infants and elderly and immunocompromised persons at the highest risk of severe complications from viral infection (1–9). No licensed therapeutics or vaccines exist to combat or prevent HMPV infection. Nearly all individuals have been exposed to HMPV by the age of 5 years (10, 11). Infection with this virus results in a neutralizing antibody (nAb) response in almost all healthy individuals, but data show that the nAb titers present in a large percentage of previously infected people are insufficient to prevent reinfection (12–14). This indicates that humoral immunity alone is insufficient for the complete protection of humans from HMPV. The mechanism by which HMPV evades the adaptive immune system is still unknown, but recent evidence suggests that impairment of the lung CD8⁺ T cell response following HMPV infection is a contributing factor (15). In contrast to humans, infection of immunocompetent mice with HMPV results in sterilizing immunity, preventing reinfection (16, 17).

HMPV, like other members of the *Paramyxoviridae* family, such as respiratory syncytial virus (RSV) and parainfluenza viruses, can subvert the innate immune response through modula-

tion of the type I interferon (IFN) signaling pathway (18, 19). Type I IFN signaling, which is initiated through activation of the IFN- α receptor (IFNAR), is thought to be integral to the early immune response through the induction of antiviral effector molecules (20–22). In addition, this pathway can modulate the adaptive immune response by contributing to both clonal expansion and maintenance of memory T cells, as well as priming and differentiation of antigen-presenting cells (APCs) (23–26).

Recent data indicate that HMPV infection generates function-

Received 10 November 2014 Accepted 28 January 2015

Accepted manuscript posted online 4 February 2015

Citation Hastings AK, Erickson JJ, Schuster JE, Boyd KL, Tollefson SJ, Johnson M, Gilchuk P, Joyce S, Williams JV. 2015. Role of type I interferon signaling in human metapneumovirus pathogenesis and control of viral replication. *J Virol* 89:4405–4420. doi:10.1128/JVI.03275-14.

Editor: D. S. Lyles

Address correspondence to John V. Williams, john.williams@vanderbilt.edu.

Copyright © 2015, American Society for Microbiology. All Rights Reserved.

doi:10.1128/JVI.03275-14

ally impaired virus-specific CD8⁺ T cells in the lungs as a result of signaling through the inhibitory receptor programmed death 1 (PD-1) (15). PD-1, along with other inhibitory receptors, has been shown to be highly upregulated in both cancer and chronic viral infections (27–29), but little is known about the role of PD-1 in acute respiratory viral infections. The ligand for PD-1, programmed death ligand 1 (PD-L1), is expressed on professional APCs, as well as primary infected lung epithelial cells, and is thought to be induced in an IFN-dependent manner (30, 31).

In this study, we used an established model of HMPV infection to demonstrate that genetic ablation of the IFN- α receptor (IFNAR^{-/-} mice) diminished the HMPV-specific CD8⁺ T cell response. We found that although IFNAR-deficient animals were able to clear the virus after infection and developed significantly higher antibody titers, they displayed less overall disease and lung inflammation than wild-type (WT) animals. Despite similar PD-1 expression levels and lower PD-L1 expression levels in IFNAR^{-/-} and WT mice during HMPV infection, HMPV-specific CD8⁺ T cells were more impaired in IFNAR^{-/-} mice than in WT mice. T cell Ig and mucin domain-containing molecule 3 (Tim-3) was significantly upregulated on HMPV-specific CD8⁺ T cells in IFNAR^{-/-} animals. Further investigation of the specific APC subsets in the lung during HMPV infection showed that alveolar macrophages do not rely on IFNAR signaling for expansion or the expression of PD-L1, but significantly fewer dendritic cells (DCs) were found in IFNAR^{-/-} mice during HMPV infection. Both DCs and interstitial macrophages upregulated PD-L1 in an IFNAR-dependent manner, while alveolar macrophages expressed higher levels of the inhibitory ligand than other lung APC subsets in both infected and uninfected WT and IFNAR^{-/-} mice.

MATERIALS AND METHODS

Mice and viruses. C57BL/6 (B6) mice were purchased from The Jackson Laboratory. IFN- α / β receptor-deficient (IFNAR^{-/-}) B6 mice were kindly provided by Herbert W. Virgin. All animals were bred and maintained under specific-pathogen-free conditions in accordance with guidelines approved by the AAALAC and the Vanderbilt Institutional Animal Care and Use Committee. Six- to 12-week-old age- and gender-matched animals were used in all experiments. HMPV (pathogenic clinical strain TN/94-49, genotype A2) was grown and titers were determined in LLC-MK2 cells as previously described (32). For all experiments, mice were anesthetized with intraperitoneally administered ketamine-xylazine and infected intranasally with 1.5×10^6 PFU of HMPV. Serum was collected from WT and IFNAR^{-/-} mice by submandibular venipuncture and used in a plaque reduction assay to determine HMPV nAb titers as previously described (32). The median values of triplicate measurements of percent HMPV neutralization for each animal of each genotype were plotted as a function of the log₂-transformed serum dilution factor and analyzed in a sigmoidal dose-response curve to determine the 50% inhibitory concentration (IC₅₀). Nasal turbinates and lungs were collected for analysis, and tissue viral titers were measured by plaque titration as previously described (32). For histopathology analysis, the left lung was removed, inflated with 10% buffered formalin, paraffin embedded, stained, and analyzed by using a formal scoring system in a group-blinded fashion by an experienced lung pathologist as previously described (15).

Pulse oximetry. To measure breath distension, mice were anesthetized with an isoflurane-oxygen (2:98%; 2 liters/min) mixture (VetEquip). Mice were secured on their backs and given constant anesthesia during the procedure via a nosecone attachment. The right leg and thigh were shaved, and a thigh sensor was secured to the right thigh of each mouse and covered with a dark cloth to reduce ambient light. A pulse oximeter (MouseOx; Starr Life Sciences Corp.) was used to measure arterial O₂ saturation, heart rate, pulse rate, pulse distension, and breath distension every 0.1 s (MouseOx software,

version 4.0). Each mouse was monitored until sufficient data were collected in which all of the parameters were successfully measured, and only these data were used in analyses (1 to 2 min per mouse). The breath distension of each animal was calculated by averaging all of the measurements for each mouse per condition per genotype.

Flow cytometry. Cells were isolated from lungs of infected animals as previously described (15). Briefly, lungs were rinsed in R10 medium (RPMI 1640 [Mediatech] plus 10% fetal bovine serum [FBS], 2 mM glutamine, 50 μ g/ml gentamicin, 2.5 μ g/ml amphotericin B, and 50 μ M β -mercaptoethanol [Gibco, Invitrogen]), minced with a scalpel, and then incubated with 2 mg/ml collagenase A (Roche) and 20 μ g/ml DNase (Roche) for 1 h at 37°C. Single-cell suspensions of digested lungs were obtained by pressing lung tissue through a steel screen (80 mesh) and then passing it over a nylon cell strainer (70- μ m pore size). Erythrocytes were lysed with Red Blood Cell Lysis Buffer (Sigma-Aldrich). For labeling of HMPV-specific CD8⁺ T cells, single-cell suspensions of mouse lungs were incubated with APC-labeled H2-D^b tetramers (0.1 to 1 μ g/ml) and anti-CD8 α (clone 53-6.7; BD Biosciences), and anti-CD19 (clone 1D3; eBioscience) antibodies (15). Surface/tetramer staining was performed for 1 h at room temperature in phosphate-buffered saline (PBS) containing 2% FBS and 50 nM dasatinib (LC Laboratories) (33). For assessment of PD-L1 expression, cells were stained with anti-epithelial cell adhesion molecule (EpCAM, clone G8.8; BioLegend), anti-CD11c (clone HL3; BD), anti-CD11b (clone M1/70; Tonbo), and anti-major histocompatibility complex (MHC) class II (clone 2G9; eBioscience) antibodies. Cells were also stained with PD-1 (clone J43; BD Biosciences), Tim-3 (clone RMT3-23), LAG-3 (clone C9B7W), 2B4 (clone m2B4 (B6)458.1; BioLegend), and PD-L1 (clone MIH5; BD) antibodies or an isotype control antibody (hamster IgG2 κ). Staining for HMPV-specific CD8⁺ T cells was normalized to the binding of a cognate APC-labeled H2-D^b tetramer loaded with influenza virus peptide NP366 to CD8⁺ T cells (typically, 0.05 to 0.2% CD8⁺ T cells). For all cell populations, forward scatter (FSC) and side scatter (SSC) gating was used to obtain cells of the appropriate size and shape.

To identify HMPV-infected cell populations, homogenized lung cell suspensions were stained with polyclonal anti-HMPV guinea pig sera (32) for 1 h at room temperature, washed, and then stained with a fluorescein isothiocyanate (FITC)-conjugated anti-guinea pig secondary antibody (Life Technologies). Lung epithelial cells and CD11c⁺ high DCs were identified by FSC and SSC and stained for EpCAM and CD11c antibodies as described above. Gates for HMPV-positive cell populations were set by using uninfected mice and isotype controls (BioLegend and BD). All flow cytometric data were collected with an LSRII flow cytometer or an LSRFortessa cell analyzer (BD Biosciences) and analyzed with FlowJo software (Tree Star).

Intracellular cytokine staining (ICS). Lung or spleen lymphocytes were isolated and restimulated *in vitro* for 6 h at 37°C with a nonspecific peptide or the indicated synthetic peptide (10 μ M final concentration) in the presence of an anti-CD107a antibody (clone 1D4B; BD Biosciences). The protein transport inhibitors brefeldin A and monensin (BD Biosciences) were added for the final 4 h of restimulation. Stimulation with phorbol myristate acetate (PMA)-ionomycin (50 ng/ml PMA and 2 μ g/ml ionomycin; Sigma) served as a positive control. After restimulation, cells were stained for surface expression of CD3 ϵ (clone 145-2C11), CD8 α , and CD19, fixed, permeabilized, stained for intracellular IFN- γ (clone XMG1.2; BD Biosciences), and analyzed by flow cytometry. Background cytokine levels following restimulation were normalized to a nonspecific peptide.

Real-time RT-PCR. A 200- μ l volume of undiluted lung homogenate from infected or uninfected IFNAR^{+/+} or IFNAR^{-/-} mice was lysed with an equal volume of RLT lysis buffer (Qiagen) and frozen at -20°C. Samples were thawed, and RNA was extracted with the MagNA Pure LC total nucleic acid isolation kit (Roche Applied Sciences) on a MagNA Pure LC by the Total NA External Lysis protocol and stored at -80°C. Real-time reverse transcription (RT)-PCR was performed with 25- μ l reaction mixtures containing 5 μ l of extracted RNA on an ABI StepOnePlus real-time PCR system (Life Technologies/Applied Biosystems) with the AgPath-ID One-Step RT-PCR kit (Life Technologies/Applied Biosystems). For PD-L1, IFN- γ , interleukin-2 (IL-2), IL-12, IL-4, and IL-10 gene expression,

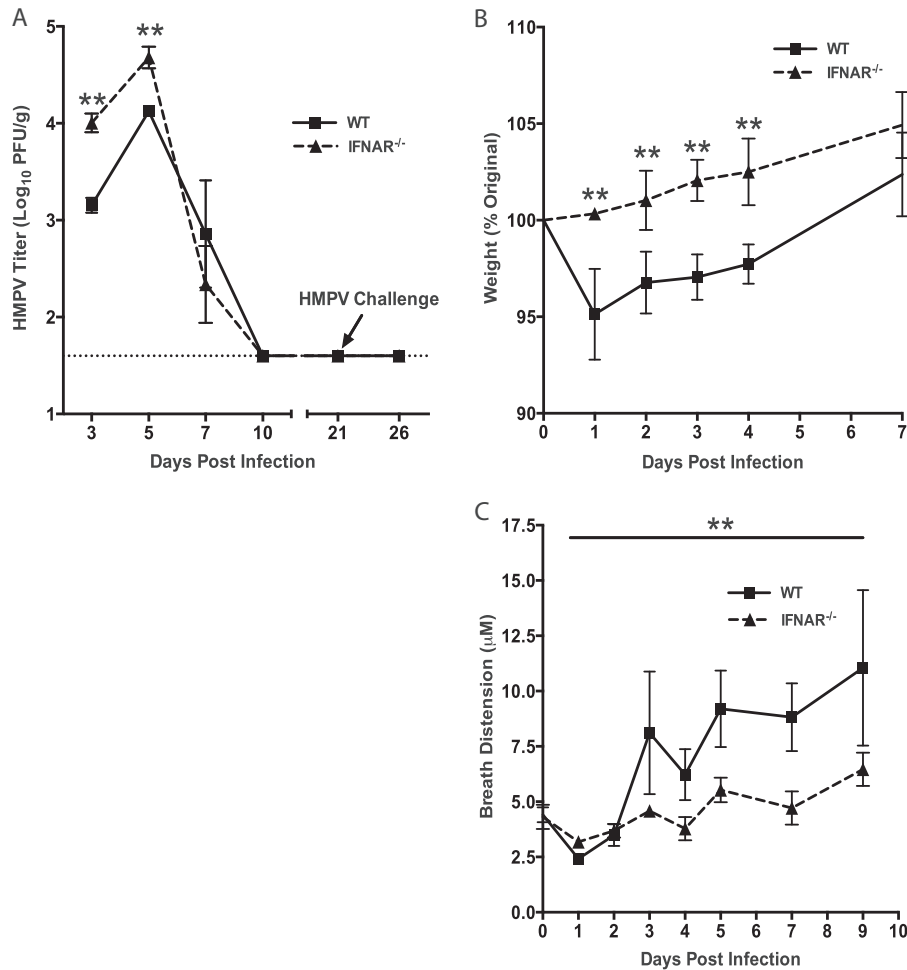


FIG 1 Type I IFN signaling limits HMPV replication but also contributes to disease pathogenesis. (A) Plaque assays were performed to measure infectious HMPV titers in the lungs of WT and IFNAR^{-/-} mice on days 3, 5, 7, and 10 postinfection. A group of mice was challenged 3 weeks after initial infection, and plaque assays were performed 5 days postinfection. $n = 9$ per group for days 3, 5, and 7; $n = 5$ per group on days 10 and 26. (B) WT and IFNAR^{-/-} mice were weighed following infection with HMPV. Data are expressed as percentages of the average original body weight in each group; error bars represent the standard error of the mean. $n = 4$ mice per group. (C) Breath distension of IFNAR^{+/+} and IFNAR^{-/-} mice was measured by pulse oximetry following HMPV infection. $n = 4$ to 10 mice per day per group with at least two independent experiments. Groups were compared by unpaired t test or two-way ANOVA. *, $P < 0.05$; **, $P < 0.02$.

exon-spanning primers and probes were used according to the manufacturer's instructions (Applied Biosystems/Ambion). All values were normalized to the hypoxanthine phosphoribosyltransferase housekeeping gene. Cytokine transcript levels were low or undetectable in uninfected IFNAR^{-/-} and WT mice. Therefore, experimental samples are reported as fold differences between HMPV-infected WT and HMPV-infected IFNAR^{-/-} mice determined by the $\Delta\Delta C_T$ method (34). Samples with cycle threshold (C_T) values of <40 were considered positive.

Statistical analyses. Data analysis was performed with Prism v4.0 (GraphPad Software). Groups were compared by unpaired t test or one-way analysis of variance (ANOVA) with a *post hoc* Tukey test for multiple comparisons. $P < 0.05$ was considered significant by convention.

RESULTS

Type I IFN signaling limits HMPV replication and spread but also contributes to disease pathogenesis. To characterize the role of IFNAR signaling in HMPV infection, we investigated the kinetics of HMPV replication in an IFNAR-deficient (IFNAR^{-/-}) transgenic mouse model. IFNAR^{-/-} mice exhibited significantly more infectious virus in the lungs at the peak of HMPV infection

(3 and 5 days postinfection) than WT controls did. However, viral clearance in IFNAR^{-/-} mice was similar to that in WT animals, with decreasing virus titers at day 7 and no detectable virus by day 10 (Fig. 1A). WT and IFNAR^{-/-} mice were challenged at 22 days postinfection, and neither had detectable viral replication.

To investigate the role of IFNAR in disease severity during HMPV infection, we first assessed weight loss and breath distension. IFNAR^{-/-} mice showed significantly less weight loss than WT mice early after infection (Fig. 1B). We used a mouse oximeter to quantify airway dysfunction, a key feature of severe LRI in humans (35). Airway dysfunction and subsequent air trapping during HMPV infection lead to pulsus paradoxus, an exaggeration of the pulse volume during respiration as a result of increased breathing effort (36), which we quantified as breath distension. IFNAR^{-/-} mice had significantly less breath distension than WT animals throughout the course of HMPV infection (Fig. 1C). Measurements of HMPV-infected IFNAR^{-/-} mice were similar to those of uninfected WT mice (not shown).

Type I IFN signaling contributes to histopathological disease during HMPV infection, and IFNAR deficiency leads to lower levels of inflammatory cytokines. To determine whether the marked lack of airway dysfunction in IFNAR^{-/-} mice corresponded to histopathological disease, the lungs of HMPV-infected WT and IFNAR^{-/-} mice and uninfected control mice were stained with hematoxylin and eosin (H&E) (Fig. 2A) and periodic acid-Schiff (PAS) stain, which preferentially stains polysaccharides in mucus (Fig. 2B). HMPV-infected WT mice had more inflammatory infiltrate than uninfected animals did, while the lung architecture of infected IFNAR^{-/-} mice appeared similar to that of uninfected controls with less inflammatory infiltrate (Fig. 2A). Additionally, there appeared to be more mucus production in the lungs of WT than IFNAR^{-/-} mice (Fig. 2B). Analysis of lung histopathology with a formal scoring system produced significantly higher inflammation scores for the WT than the IFNAR^{-/-} groups (Fig. 2C). We also measured cytokine levels from whole lung homogenates collected from HMPV-infected, as well as uninfected, WT and IFNAR^{-/-} mice by RT-PCR. In uninfected animals, these cytokines were undetectable by this assay or present at very low levels (data not shown). Therefore, we compared infected WT and IFNAR^{-/-} mice. These analyses revealed that the levels of the TH₁ cytokines IFN- γ , IL-2, and IL-12 were lower in HMPV-infected IFNAR^{-/-} mice than in HMPV-infected WT mice (Fig. 2C), while the TH₂ cytokine IL-4 levels in the infected WT and infected IFNAR^{-/-} groups were not different. Together, these data suggest that IFNAR signaling contributes to disease pathogenesis in the lungs of HMPV-infected mice.

Lack of type I IFN signaling does not change CD8⁺ T cell, CD19⁺ B cell, or CD11c⁺ cell infiltration during HMPV infection. The cytokine data suggested a deficiency in the adaptive cellular immune response to HMPV infection in IFNAR^{-/-} mice. To test the hypothesis that IFNAR signaling promotes adaptive immune responses to HMPV, we assessed nAb titers and examined immune cells known to be important in the host response to respiratory viruses in the lungs of WT and IFNAR^{-/-} mice. Twenty-one days after HMPV infection, serum was collected from previously infected WT and IFNAR^{-/-} mice, and plaque neutralization assays were performed. IFNAR^{-/-} mice possessed significantly higher nAb titers than WT mice (Fig. 3A), but, as indicated in Fig. 1, both groups were immune to reinfection.

Next, we examined the infiltration of the infected lung by immune cells. Ten days after HMPV infection, at the peak of the adaptive response, the total numbers of lymphocytes in the lungs of WT and IFNAR^{-/-} mice were not significantly different (Fig. 3B). Counts of CD11c⁺ high lung cells, which are important for induction of innate and adaptive immune responses via viral antigen presentation, were significantly higher in both IFNAR^{-/-} and WT mice at 10 days postinfection than in uninfected controls. However, no statistically significant difference in CD11c⁺ high cell numbers between IFNAR^{-/-} and WT mice was noted (Fig. 3C). Neither CD8⁺ T cell nor CD19⁺ B lymphocyte levels were significantly different in HMPV-infected mice when measured as a percentage of the total lymphocyte population after HMPV infection in WT or IFNAR^{-/-} animals (Fig. 3D; data not shown). These data suggest that IFNAR signaling is not crucial for the recruitment of adaptive immune cells to the site of HMPV infection.

Efficient development of a functional HMPV-specific CD8⁺ T cell response requires type I IFN signaling. Given diminished respiratory tract pathology in IFNAR^{-/-} mice (Fig. 1 and 2) but

similar recruitment of inflammatory cells to the lungs (Fig. 3) upon HMPV infection, we wondered whether the functionality of the cells that reach the lungs of IFNAR^{-/-} mice differs from that of their counterparts in WT mice. To test this hypothesis, we first quantified the virus-specific component of the adaptive immune response. To do this, we performed MHC tetramer staining for the immunodominant HMPV epitope F₅₂₈₋₅₃₆ (F528) to enumerate HMPV epitope-specific cells. IFNAR^{-/-} mice had significantly fewer F528-specific CD8⁺ T cells in the lungs than WT animals did (Fig. 4A). Next, we examined the functionality of these HMPV-specific cells by *ex vivo* peptide stimulation and ICS of lung lymphocytes collected 10 days postinfection. A significantly smaller fraction of HMPV-specific CD8⁺ T cells from IFNAR^{-/-} mice produced IFN- γ than those from WT mice (Fig. 4B). On the basis of previous studies showing that PD-1 signaling contributes to T cell impairment (15), we quantified PD-1 expression on both HMPV-specific and total CD8⁺ T lymphocytes. Although PD-1 was upregulated on HMPV-specific CD8⁺ T cells compared to that on bulk CD8⁺ T cells following viral infection, PD-1 expression on these HMPV-specific T cells was similar in IFNAR^{-/-} and WT animals (Fig. 4C). These data indicate an important role for type I IFN signaling in the development of functional pulmonary CD8⁺ T cells and show that the absence of IFNAR signaling does not directly affect PD-1 expression on CD8⁺ T cells, consistent with prior studies demonstrating T cell receptor signaling as the primary determinant of PD-1 expression (15).

Type I IFN signaling limits the spread of HMPV in lung epithelial cells. To further examine the infected lung epithelium in the mouse model, we developed an assay for the isolation and analysis of lung epithelial cells by flow cytometry. The average number of HMPV-infected lung cells in IFNAR^{-/-} and WT mice was analyzed by using a monoclonal antibody to identify EpCAM⁺ lung epithelial cells and a polyclonal anti-HMPV serum to identify HMPV⁺ EpCAM⁺ cells (Fig. 5A). IFNAR^{-/-} animals had a significantly higher percentage of HMPV⁺ EpCAM⁺ lung epithelial cells on day 5 postinfection (Fig. 5B). No viral antigen was detected by flow cytometry in epithelial cell populations at 10 days postinfection or in CD11c⁺ high lung DCs at either 5 or 10 days postinfection (data not shown). These data show that type I IFN is important in controlling not only replication, as shown in Fig. 1, but also viral spread in the lung.

Expression of PD-L1 is driven by, but not dependent on, type I IFN signaling in lung epithelial cells and CD11c⁺ cells. Since the expression of PD-1 was not different on virus-specific IFNAR^{-/-} and WT cytotoxic T lymphocytes (CTLs), we wondered whether the differences in CTL functionality we observed could be due to altered expression of the PD-1 ligand PD-L1. Prior work has indicated that the promoter of PD-L1 contains IFN regulatory elements and that IFN signaling can promote PD-L1 expression on epithelial and endothelial cells (37, 38). We therefore quantified the expression of PD-L1 in respiratory epithelial cells and CD11c high cells on day 5 after HMPV infection. PD-L1 was significantly upregulated on both virus antigen-positive and virus antigen-negative lung epithelial cells in both WT and IFNAR^{-/-} mice (Fig. 6A). However, PD-L1 expression was significantly lower in IFNAR^{-/-} animals than in WT animals. By 10 days postinfection, no differences in the levels of PD-L1 expression in lung epithelial cells in HMPV-infected WT and IFNAR^{-/-} mice (Fig. 6B) or in total PD-L1 transcript levels in the lungs of these animals (data not shown) were observed, although the PD-L1 lev-

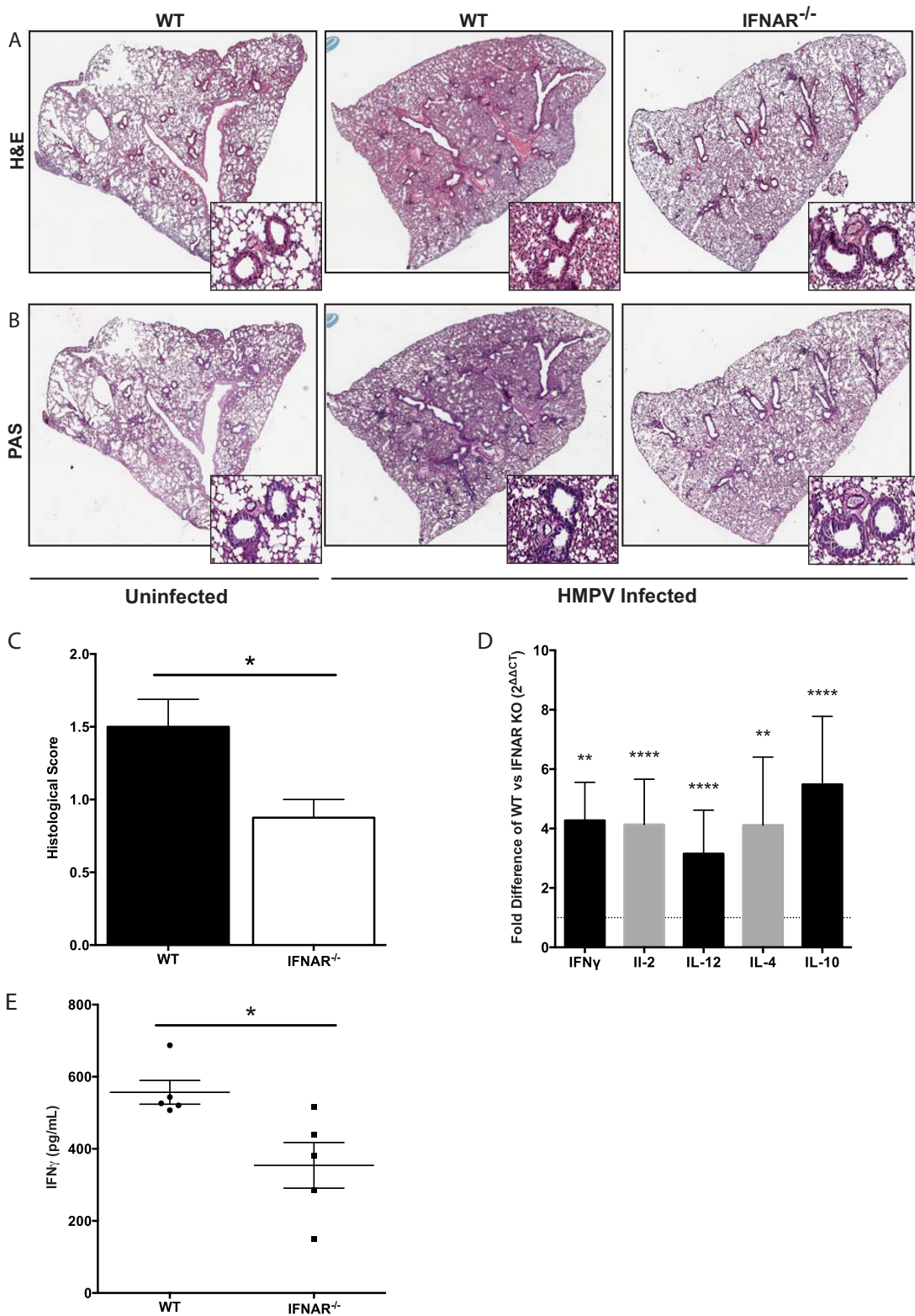


FIG 2 Type I IFN signaling contributes to histopathological disease during HMPV infection, and IFNAR deficiency leads to lower levels of inflammatory cytokines. Lungs from WT and IFNAR^{-/-} mice 5 days after HMPV infection or uninfected control animals were stained with H&E (A) or PAS stain (polysaccharide specific) (B). Images of whole lungs from WT and knockout animals were taken at a magnification of $\times 1$ with an Aperio ImageScope slide scanner. Representative lung images at a magnification of $\times 20$ are shown in the insets. (C) Lung sections were scored by a board-certified pathologist. $n = 8$ mice per group. (D) At 7 days postinfection, lungs were harvested and cytokine levels were measured by RT-PCR. Data are results of a $\Delta\Delta C_T$ analysis of IFNAR^{-/-} and WT groups. $n = 8$ mice per group. (E) At 7 days postinfection, lungs were harvested and IFN- γ levels were determined by enzyme-linked immunosorbent assay. $n = 5$ mice per group. Error bars represent the standard error of the mean. *, $P < 0.05$; **, $P < 0.02$; ****, $P < 0.0001$.

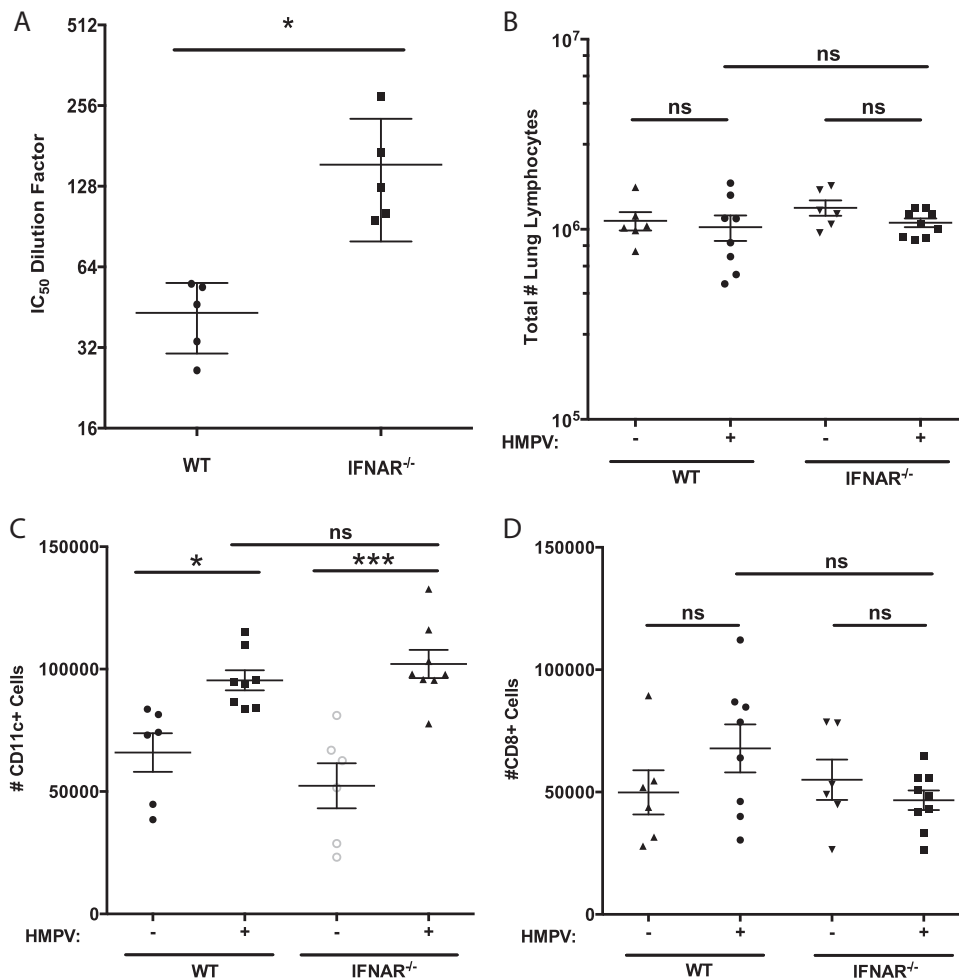


FIG 3 Lack of type I IFN signaling leads to higher serum nAb titers and does not change CD8⁺ T cell or CD11c⁺ DC infiltration during HMPV infection. WT B6 mice and IFNAR knockout mice were infected with 10⁶ PFU of HMPV, and at 21 days postinfection, these animals were submandibularly bled and their serum was harvested. *In vitro* neutralization assays of LLC-MKC cells were performed in triplicate with increasing dilutions of previously infected mouse serum to determine the IC₅₀ in serum. (A) Median percent neutralization values ($n = 5$ per group) were plotted as a function of the serum dilution factor to obtain best-fit curves, and the IC₅₀ was calculated for each curve. Lungs of WT and IFNAR^{-/-} mice 5 (C) or 10 (B, D) days after HMPV infection or uninfected control animals were harvested and analyzed by flow cytometry. (A) Cells were gated on the small lymphocyte population, and the infiltration of these cells is shown as the total number of lung lymphocytes. Specific staining of CD11c (C) and CD8 (D) allowed the enumeration of CD8⁺ T cells and CD11c⁺ DCs. Total lung cell values, used to calculate the number of cells, were measured by hemocytometer. Groups were compared by unpaired *t* test or one-way ANOVA with a *post hoc* Tukey test where appropriate. $n = 4$ to 15 mice per group with at least two independent experiments. Error bars represent the standard error of the mean. *, $P < 0.05$; **, $P < 0.02$; ***, $P < 0.002$; ns, not significant.

els on epithelial cells were still significantly higher in both groups than on those of uninfected mice. These results indicate that while IFNAR signaling can lead to increased expression of PD-L1, it is not an exclusive regulator of this ligand and other signaling pathways can upregulate PD-L1.

PD-L1 expression on bulk CD11c⁺ lung cells 5 days after HMPV infection in both WT and IFNAR^{-/-} mice was slightly greater than that in uninfected animals, but the difference did not reach significance and no difference between groups was detected (Fig. 6C). On day 10 postinfection, PD-L1 expression on CD11c⁺ cells was indistinguishable between infected and uninfected WT and IFNAR^{-/-} mice (Fig. 6D). Later analyses of the subsets of CD11c⁺ cells in the lungs (see Fig. 9 and 10) demonstrated that, in fact, this population of cells is heterogeneous and the discrete APC subsets in this gate have significant differences in their baseline

expression of PD-L1 and the upregulation of this inhibitory ligand upon HMPV infection.

Functional impairment of HMPV-specific CD8⁺ T cells is not due to Treg cell infiltration but rather corresponds to expression of the inhibitory receptor Tim-3. IFNAR signaling has been shown to affect the development and recruitment of CD4⁺ regulatory T (Treg) cells, but the data are unclear as to whether that effect is positive or negative (39–42). Treg cells possess a myriad of anti-inflammatory properties, including suppression of virus-specific CTLs during LRI (43). We therefore quantified Treg cell infiltration of the lungs of infected IFNAR^{-/-} and WT mice at day 5 after HMPV infection. We found significant Treg cell infiltration in the lungs of infected WT mice but not in those of IFNAR^{-/-} animals (Fig. 7A). These results help explain the lower IL-10 transcript level we observed in IFNAR^{-/-} mice than in WT

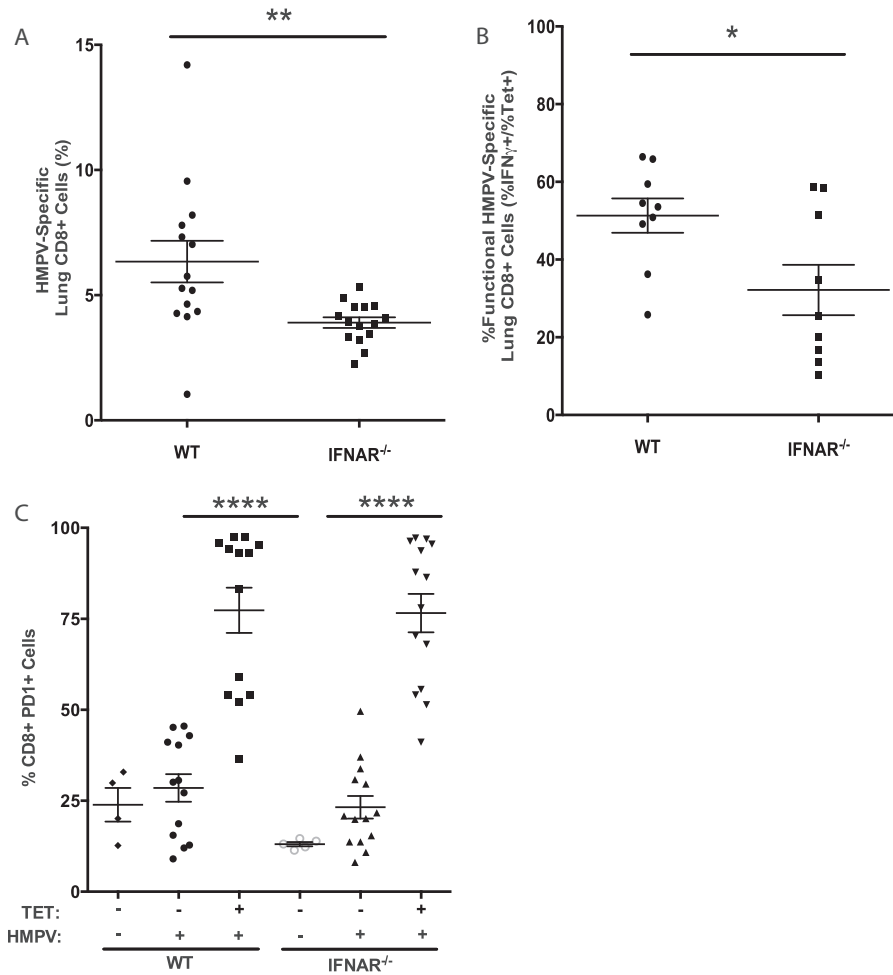


FIG 4 Efficient development of a functional HMPV-specific CD8⁺ T cell response requires type I IFN signaling. WT and IFNAR^{-/-} mice were infected with HMPV, and lungs were harvested at 10 days postinfection and analyzed by flow cytometry. (A) An HMPV-specific tetramer molecule was used to probe for virus-specific CD8⁺ T cells in infected lungs for both groups. (B) Lymphocytes were also stimulated with an HMPV peptide *in vitro*, and ICS was performed to analyze the functionality of HMPV-specific T cells. (C) An antibody specific for the inhibitory receptor PD-1 was used to examine its expression on bulk CD8⁺ T cells in infected and uninfected animals and on HMPV-specific CD8⁺ T cells from infected mice. Groups were compared by unpaired *t* test or one-way ANOVA with a *post hoc* Tukey test where appropriate. *n* = 9 to 15 mice from at least two independent experiments per group. Error bars represent the standard error of the mean. *, *P* < 0.05; **, *P* < 0.02; ****, *P* < 0.0001. TET, tetramer.

mice (Fig. 2D) and suggest that IFNAR signaling is important for Treg cell infiltration during HMPV infection. However, recruitment of Treg cells does not appear to be responsible for the impaired CD8⁺ T cell phenotype. We analyzed HMPV-specific CD8⁺ T cells 10 days postinfection for the expression of the other known inhibitory receptors Tim-3, LAG-3, and 2B4. Significant upregulation of 2B4 (Fig. 7B) was observed on HMPV-specific CD8⁺ T cells, although there were no differences between WT and IFNAR-deficient mice. No significant upregulation of LAG-3 (Fig. 7C) was observed on HMPV-specific CD8⁺ T cells in either IFNAR^{-/-} or WT animals. However, we found that the percentage of Tim-3⁺ HMPV-specific CD8⁺ T cells was significantly higher in IFNAR^{-/-} mice than in WT mice (Fig. 7D). There were significantly more Tim-3⁺ HMPV-specific CD8⁺ T cells in both IFNAR^{-/-} and WT mice than in either naive CD8⁺ T cells from uninfected animals or nonspecific CD8⁺ T cells from HMPV-infected WT mice (Fig. 7D). These data indicate that upregulation of the inhibitory receptor Tim-3 is associated with an exhausted

phenotype observed in HMPV-specific CD8⁺ T cells in the context of IFNAR deficiency.

Subsets of lung APCs are differentially affected by IFNAR signaling during HMPV infection. Four distinct categories of APCs located in the mouse lung have been classified on the basis of their surface marker expression (Fig. 8), as well as their ability to present viral epitopes to CD8⁺ T cells during infection (44). Both alveolar macrophages and DCs (Fig. 8, top right) express high levels of CD11c but can be distinguished from each other by the higher level of MHC class II expression in the DC subset (45). DCs in the lungs can also be broken down into two groups, CD11b⁺ and CD11b⁻ DCs (Fig. 8, bottom right), which have also been shown to express CD103 (46; data not shown). Interstitial macrophages (Fig. 8, bottom left) in the lung do not express CD11c but do express high levels of CD11b and moderate levels of MHC class II.

During HMPV infection, both WT and IFNAR^{-/-} mice display significantly more alveolar macrophages than uninfected animals in each group do (Fig. 9A), but the number of DCs

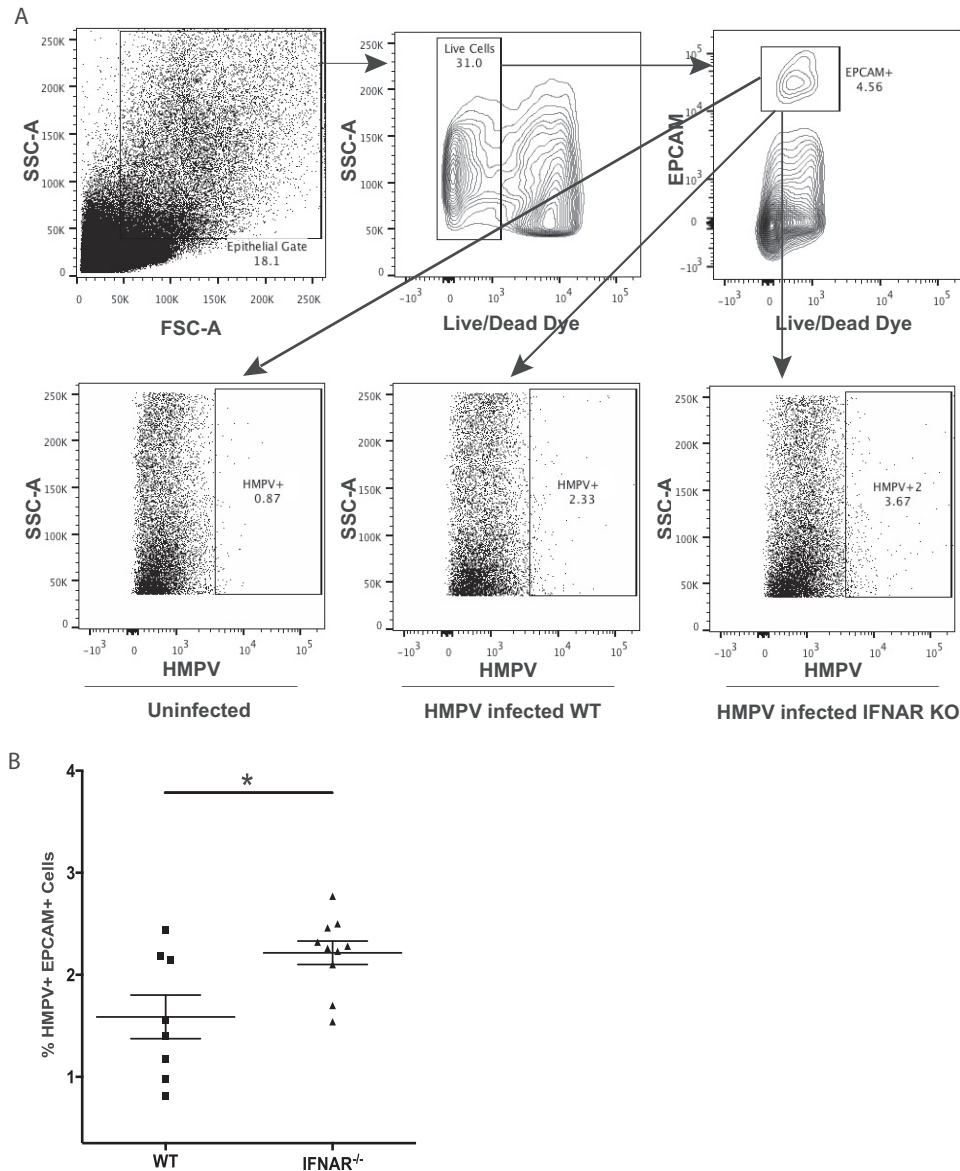


FIG 5 Type I IFN limits the spread of HMPV in lung epithelial cells. (A) Cells were stained for EpCAM and HMPV. Dead cells were excluded with an amine-reactive dye. All analysis was done directly *ex vivo*. For analysis of HMPV⁺ EpCAM⁺ cells, background staining of HMPV for uninfected mouse lung cells was determined and subtracted from experimental values. For analysis of PD-L1 expression, cells were probed with an isotype control antibody and this background was subtracted from experimental values. (B) At day 5 after HMPV infection, lungs were harvested and stained for EpCAM-positive lung epithelial cells. These cells were then probed for HMPV antigen with a polyclonal antibody and a fluorescent secondary antibody, and the percentage of HMPV-infected EpCAM⁺ cells in each group was measured by flow cytometry. $n = 4$ to 10 mice per day per group with at least two independent experiments. Groups were compared by unpaired *t* test or two-way ANOVA. *, $P < 0.05$.

proved to be IFN dependent, as the number of DCs in the lungs of infected IFNAR^{-/-} animals equaled the number in uninfected mice and was significantly lower than that in HMPV-infected WT mice (Fig. 9B). In addition, significantly more CD11b⁺ DCs were present in the lungs of HMPV-infected WT mice than in uninfected WT or IFNAR^{-/-} mice and infected IFNAR^{-/-} mice (Fig. 9C). No significant differences in the number of CD11b⁻ DCs (Fig. 9D) or interstitial macrophages in uninfected and infected or WT and IFNAR^{-/-} mice (Fig. 9E) were seen. These data show that type I IFN is crucial for the recruitment and/or proliferation of DCs in infected mouse

lungs but that alveolar macrophages are unaffected by a lack of IFNAR signaling during HMPV infection.

IFNAR signaling affects the expression of PD-L1 on DCs and interstitial macrophages, but alveolar macrophages constitutively express high levels of PD-L1 regardless of the presence of IFNAR. To determine the ability of various subtypes of lung APCs to signal through the inhibitory PD-1–PDL-1 pathway, we analyzed the fraction of cells expressing the inhibitory ligand PD-L1 during HMPV infection. We found that nearly all of the alveolar macrophages in uninfected and infected WT and IFNAR^{-/-} mice expressed PD-L1 (Fig. 10A). Conversely, the percentage of cells

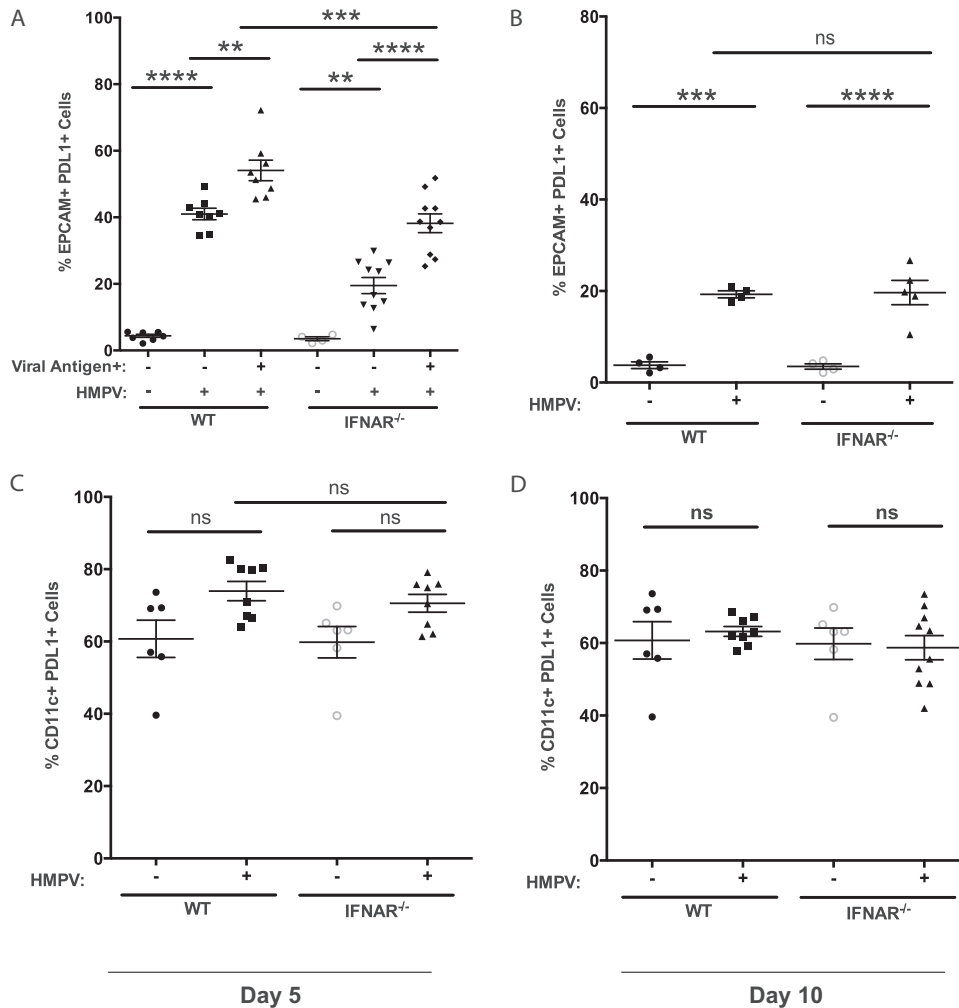


FIG 6 Expression of PD-L1 is driven by, but not dependent on, type I IFN signaling in lung epithelial cells and CD11c⁺ DCs. WT and IFNAR^{-/-} mice were infected with HMPV, and at 5 (A, C) or 10 (B, D) days postinfection, their lungs were harvested along with uninfected control mouse lungs (HMPV⁻) and analyzed by flow cytometry. Specific staining of EpCAM (A, B) and CD11c (C, D) allowed the analysis of EpCAM⁺ lung epithelium and CD11c⁺ DCs. EpCAM⁺ cells at day 5 were also probed for HMPV antigen with a polyclonal antibody and a fluorescent secondary antibody to enable gating of infected (HMPV Antigen⁺) and uninfected (HMPV Antigen⁻) cells. An antibody specific for the inhibitory ligand PD-L1 was used to measure its expression on all epithelial and DC populations at each time point. Groups were compared by unpaired *t* test or one-way ANOVA with a *post hoc* Tukey test where appropriate. *n* = 4 to 9 mice per experimental group representative of at least two independent experiments. Error bars represent the standard error of the mean. *, *P* < 0.05; **, *P* < 0.02; ***, *P* < 0.002; ****, *P* < 0.0001; ns, not significant.

expressing PD-L1 on both DC subsets, as well as interstitial macrophages, during HMPV infection was significantly lower in infected IFNAR^{-/-} mice (Fig. 10B to D). In DCs and interstitial macrophages of WT mice, a significantly greater fraction of PDL1⁺ cells was observed in HMPV-infected mice than in uninfected mice, but upregulation of PD-L1 appears to be IFNAR dependent, as IFNAR^{-/-} mice displayed no difference in PD-L1 expression on these cells during infection (Fig. 10B to D). Additionally, the level of PD-L1 expression on alveolar macrophages, as measured by mean fluorescence intensity, was significantly higher than that on the other APC subsets (Fig. 10E). Type I IFN appears to be indispensable for PD-L1 expression on DCs and interstitial macrophages during HMPV infection, but these data suggest that alveolar macrophages constitutively express this inhibitory ligand at high levels in both uninfected and infected lungs.

DISCUSSION

We investigated early and late immune responses in IFNAR-deficient mice to elucidate the effect of IFNAR deficiency on the control and clearance of this virus *in vivo*. These data demonstrate that IFNAR signaling contributes to the limitation of both the replication and the spread of HMPV, similar to what has been observed in related viruses (47–50). One group found that both type I and II IFNs are important for RSV in BALB/c mice (50, 51). IFNAR^{-/-} mice displayed significantly higher levels of infectious virus and more HMPV antigen⁺ lung epithelial cells. By 10 days after HMPV infection, virus was not detectable by either plaque assays or direct staining of lung epithelial cells. We were not able to detect any HMPV⁺ CD11c⁺ lung macrophages/DCs at either 5 or 10 days after HMPV infection. IFNAR^{-/-} mice were immune to an HMPV

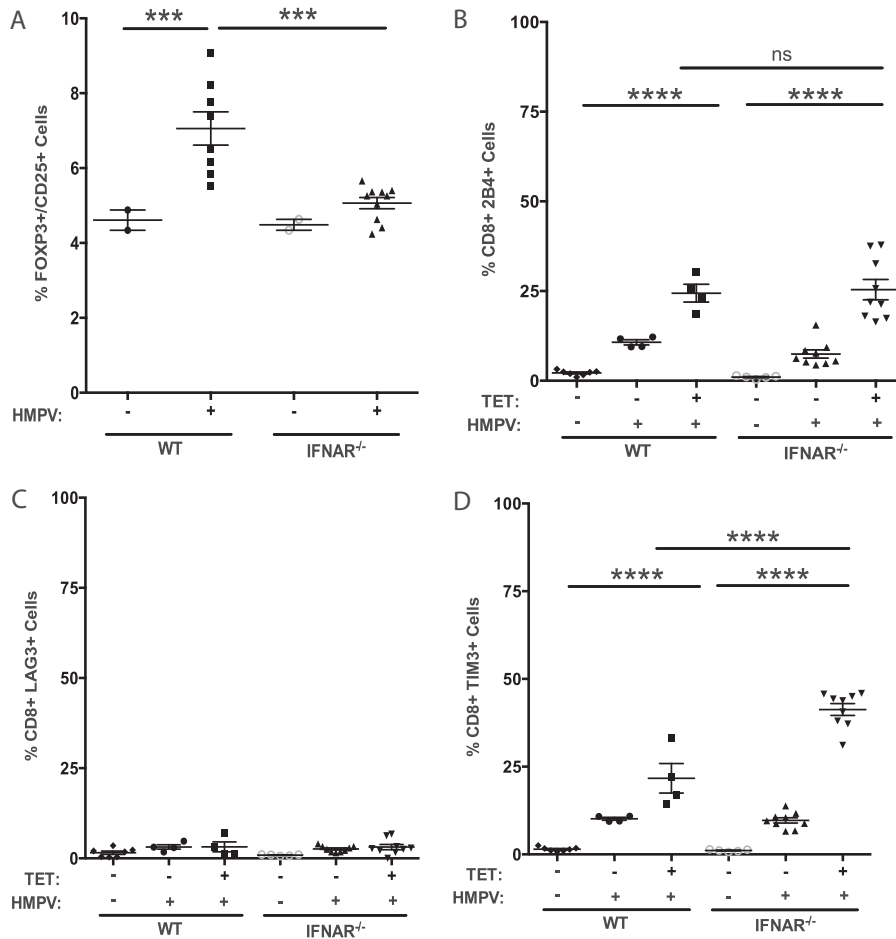


FIG 7 Functional impairment of HMPV-specific CTLs is not due to Treg cell infiltration or the expression of 2B4 or LAG-3 but rather corresponds to the expression of inhibitory receptor Tim-3. WT and IFNAR^{-/-} mice were infected with HMPV, and at 5 (A) or 10 (B, C, D) days postinfection, their lungs were harvested and analyzed by flow cytometry. (A) To identify CD4⁺ Treg cells, antibodies specific for CD4, FOXP3, and CD25 were used in uninfected and infected mice. Specific staining of bulk CD8⁺ T cells in uninfected and infected mice and HMPV-specific CD8⁺ T cells in infected animals with antibodies to the inhibitory markers 2B4 (B), LAG-3 (C), and Tim-3 (D) was used to determine percentages of inhibitory-receptor-positive cells in HMPV-specific, as well as nonspecific, CD8⁺ T cells. Groups were compared by one-way ANOVA with a *post hoc* Tukey test. $n = 4$ or 5 mice per experimental group with one independent experiment. Error bars represent the standard error of the mean. ***, $P < 0.002$; ****, $P < 0.0001$; ns, not significant.

challenge after primary infection and had a higher serum nAb titer than WT mice. This nAb titer increase could be due to increased viral antigen in IFNAR^{-/-} mice and potentially highlights an advantage of a more finely tuned modulator of the type I IFN pathway in using host innate immunity to prevent antigen loads from reaching levels necessary to develop sterilizing immunity. Moreover, these data show that, in this model, type I IFN is not required to develop a fully protective response.

Recent studies have shown that RSV infection of IFNAR-deficient mice leads to lower levels of inflammatory cytokines (52–54), and our data show that, similarly, IFNAR^{-/-} mice infected with HMPV have fewer inflammatory cytokine transcripts. Histological analysis of infected animals showed significantly less lung inflammation in IFNAR^{-/-} mice than in WT mice, and IFNAR^{-/-} mice had significantly less lung dysfunction and weight loss during infection, suggesting that IFNAR signaling contributes substantially to the major disease symptoms associated with HMPV infection (1, 9, 55). Thus, although IFNAR signaling suppresses early viral replication, it is not essential for clearance of HMPV and contributes to disease pathogenesis. A recent

paper that focused on the response to HMPV in neonatal mice deficient in important adaptors of the innate cytokine response, IPS-1, IRF3, and IRF7, also corroborates our findings regarding the importance of the balance between protection and immune-induced pathogenesis for type I IFN (56).

IFNAR^{-/-} mice had a significant defect in the number of HMPV-specific CD8⁺ T cells, consistent with previous data suggesting that IFNAR signaling plays a role in the clonal expansion of CD8⁺ T cells (25) and in the maturation and priming of APCs (26, 57–59). Virus-specific CD8⁺ T cells become functionally impaired in the lungs during acute viral LRI, including HMPV, and this functional defect is driven predominantly by inhibitory signaling from the PD-1 receptor and its ligand, PD-L1 (15). Because IFNs have been identified as inducing expression of PD-L1 (30, 37, 38), we expected to observe restoration of T cell functionality in our IFNAR^{-/-} model. However, we found that the functional impairment of CD8⁺ T cells in IFNAR^{-/-} mice was actually significantly increased. Importantly, this difference in impairment was not associated with increased expression of PD-1. In addition, while PD-L1 expression levels in the lung were upregulated in

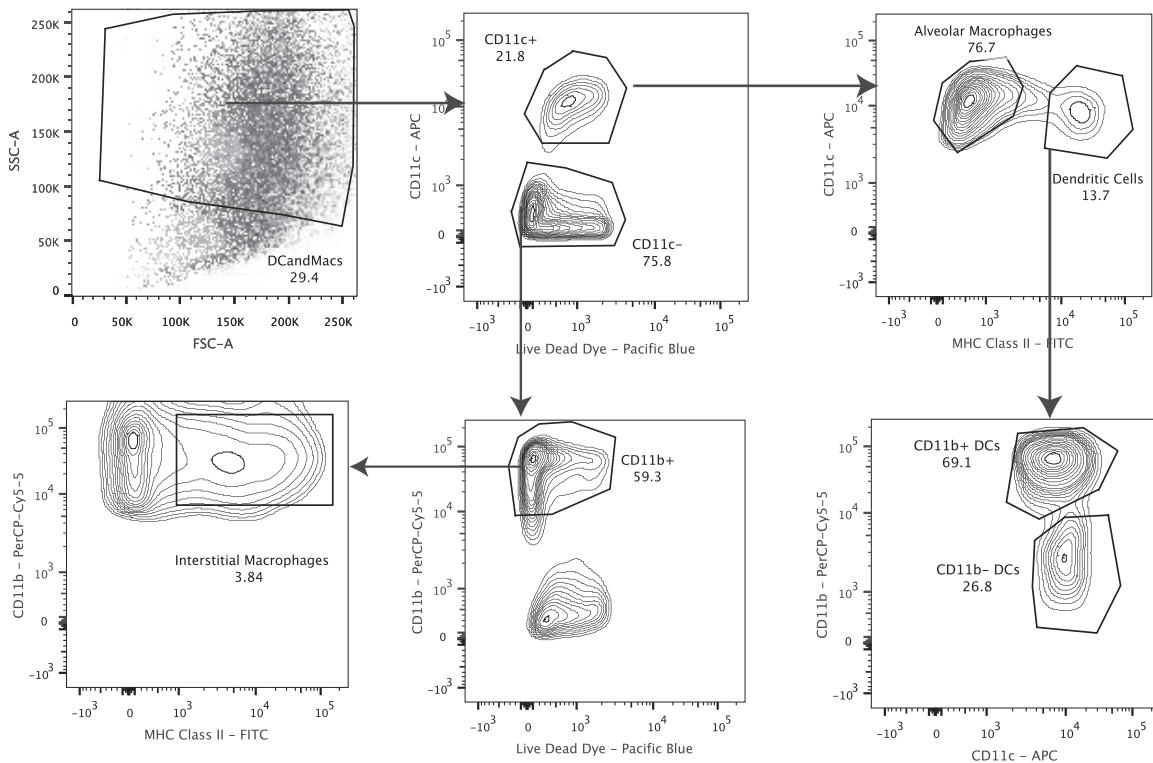


FIG 8 Gating strategies for DC and macrophage analysis. Cells were stained with CD11c, CD11b, and MHC class II. Dead cells were excluded with an amine-reactive dye. All analysis was done directly *ex vivo*. For analysis of PD-L1 expression, cells were probed with an isotype control antibody and this background was subtracted from experimental values.

both WT and IFNAR^{-/-} mice, IFNAR^{-/-} animals exhibited lower PD-L1 levels than WT animals did in both lung epithelial and CD11⁺ cells. Thus, although PD-L1 expression on both lung epithelial and CD11c⁺ cells was affected by IFNAR signaling, these differences were not sufficient to explain the reduction in the CD8⁺ T cell functionality observed in IFNAR^{-/-} mice.

To date, there are conflicting studies on the impact of IFNAR signaling on Treg cells. Some groups have shown a negative impact of IFNAR signaling on the development of Treg cells (39, 40), but others have shown that treatment with type I IFN can lead to higher Treg cell numbers (41, 42). Treg cells can secrete suppressive cytokines, such as IL-10, to limit the functionality of CD4⁺ and CD8⁺ T lymphocytes during respiratory viral infections (43), but we actually observed fewer Treg cells and lower IL-10 gene expression in IFNAR^{-/-} mice, indicating a positive role for IFNAR signaling in Treg cell recruitment or proliferation.

Other inhibitory T cell receptors, including LAG-3 (60), 2B4 (61), and Tim-3 (62), contribute to CD8⁺ T cell exhaustion during chronic infection, with the expression of multiple receptors increasing the exhaustion phenotype (63, 64). While we saw no differences in LAG-3 and 2B4 expression during HMPV infection, HMPV-specific CD8⁺ T cells from IFNAR^{-/-} mice were significantly more likely to express the Tim-3 receptor. Tim-3 is a member of the Tim family of molecules containing an N-terminal IgV domain, a mucin domain, a transmembrane domain, and a tail extending to the cytoplasm (65). This molecule is capable of binding to its ligand, galectin-9, and inducing suppressive signals in both CD4⁺ and CD8⁺ T cells (66–68). This interaction has been associated with peripheral tolerance (69). Recent studies have re-

vealed the importance of Tim-3 in cancer (27, 29) and chronic viral disease (28, 70–74). Our data show that, in the context of respiratory viral infections, the diminished function of HMPV-specific CD8⁺ T cells in IFNAR-deficient mice corresponds to increased expression of the inhibitory receptor Tim-3. Since HMPV and other viruses display the ability to downregulate IFNAR signaling, Tim-3 may provide an attractive target for therapeutic intervention during HMPV infection.

Alveolar macrophages and DCs both express the cell surface marker CD11c, and these cell types, along with interstitial macrophages, are crucial APCs in the lung (44). In WT mice, we observed an increase in both alveolar macrophages and DCs during HMPV infection, but in mice lacking IFNAR signaling, there was a significant defect in the amount of DCs, but not alveolar macrophages, in the lungs during infection. Analysis of PD-L1 expression in these subsets indicated that alveolar macrophages constitutively express high levels of this inhibitory ligand, while DCs and interstitial macrophages rely on IFNAR signaling for PD-L1 expression. Reflecting this, the total PD-L1 expression level was significantly lower in DCs and interstitial macrophages from IFNAR^{-/-} mice than in those from WT mice. Thus, the defect in the number of PD-L1^{low} DCs during viral infection of IFNAR^{-/-} mice leads to a greater ratio of APCs expressing high levels of PD-L1 (i.e., alveolar macrophages) in infected lungs, potentially explaining the decrease in CD8⁺ T cell functionality observed in IFNAR^{-/-} mice. Further, the decrease in total APCs was consistent with the defect in HMPV-specific CD8⁺ T cell numbers, suggesting a global effect of the lack of type I IFN. Additionally, our data suggest that, because of intrinsic differences in PD-L1 expres-

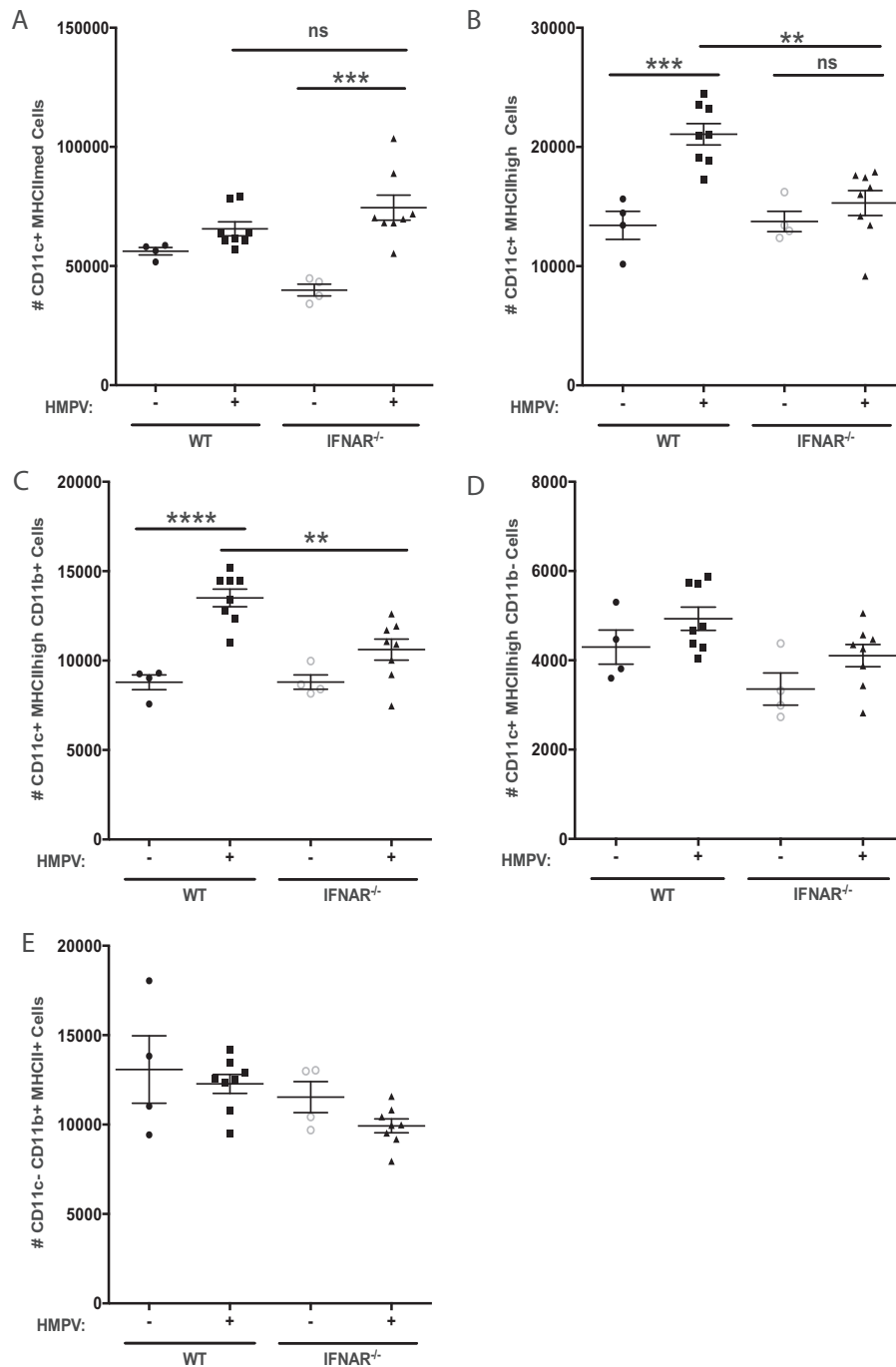


FIG 9 Subsets of lung APCs are differentially affected by type I IFN signaling during HMPV infection. WT and IFNAR^{-/-} mice were infected with HMPV, and at 5 days postinfection, their lungs were harvested and analyzed by flow cytometry. Cells were gated as CD11c⁺ MHC class II^{mid} alveolar macrophages (A, E), CD11c⁺ MHC class II^{high} CD11b⁺ DCs (B, E), CD11c⁺ MHC class II^{high} CD11b⁻ DCs (C, E), and CD11c⁻ MHC class II^{mid} CD11b⁺ interstitial macrophages (D, E). Total lung cell values, used to calculate numbers of cells, were measured by hemocytometer. Groups were compared by unpaired *t* test or one-way ANOVA with a *post hoc* Tukey test where appropriate. *n* = 4 to 9 mice per experimental group representative of at least two independent experiments. Error bars represent the standard error of the mean. *, *P* < 0.05; **, *P* < 0.02; ***, *P* < 0.002; ****, *P* < 0.0001; ns, not significant.

sion, DCs produce a more functional CD8⁺ T cell response than alveolar macrophages do. These data corroborate previous findings on the importance of DCs for the immune response in the respiratory tract (75).

It should be noted that these experiments used the B6 mouse

model for HMPV infection. This model is well established as a good one for viral replication and the development and assessment of adaptive immune responses (15, 76), but other groups studying HMPV use the BALB/c mouse model, and some differences do exist (77, 78). Specifically related to T cell polarization,

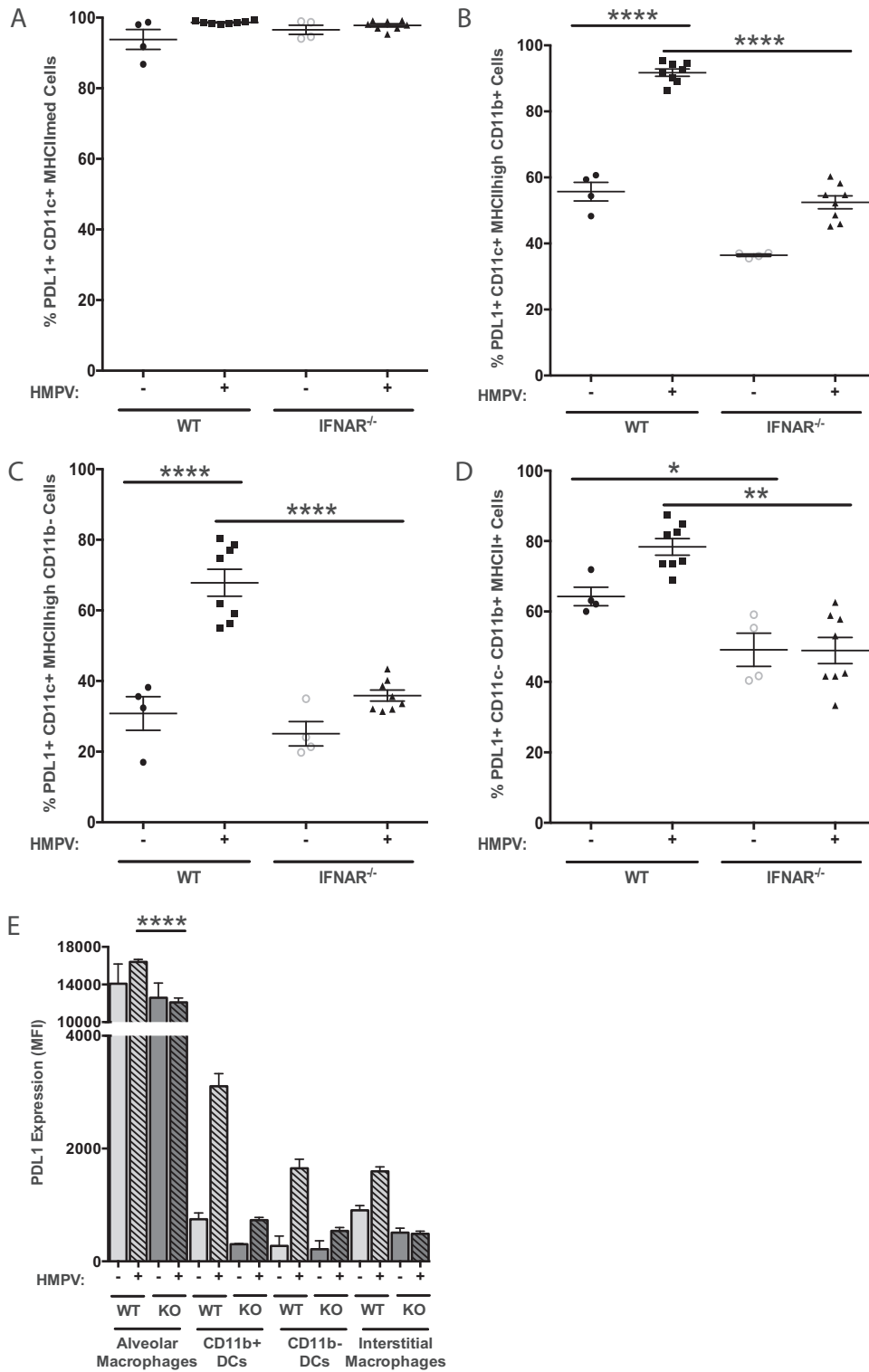


FIG 10 Type I IFN signaling drives the expression of PDL1 on DCs and interstitial macrophages, but alveolar macrophages constitutively express high levels of PDL1. WT and IFNAR^{-/-} mice were infected with HMPV, and at 5 days postinfection, their lungs were harvested and analyzed by flow cytometry. CD11c⁺ MHC class II^{mid} alveolar macrophages (A, E), CD11c⁺ MHC class II^{high} CD11b⁺ DCs (B, E), CD11c⁺ MHC class II^{high} CD11b⁻ DCs (C, E), and CD11c⁻ MHC class II^{mid} CD11b⁺ interstitial macrophages (D, E) were probed with an antibody specific for the inhibitory ligand PD-L1. An isotype control antibody was used to draw gates to measure the percentage of cells expressing this marker (A to D), as well as to normalize its expression level on four subtypes of lung APCs (E). KO, knockout. Groups were compared by unpaired *t* test or one-way ANOVA with a *post hoc* Tukey test where appropriate. *n* = 4 to 9 mice per experimental group representative of at least two independent experiments. Error bars represent the standard error of the mean. *, *P* < 0.05; **, *P* < 0.02; ***, *P* < 0.0001. MFI, mean fluorescence intensity.

B6 mice have a TH1 bias, dominated by the expression of IFN- γ , IL-2, and TNF- α , while BALB/c mice show a TH2 bias marked by the expression of IL-4, IL-5, IL-6, IL-9, IL-10, and IL-13 along with a strong antibody response (79–81). Both of these models have provided valuable information that has contributed to our understanding human disease, but the differences should be taken into consideration.

Taken together, our data reveal an important role for type I IFN signaling in both the innate and adaptive host control of HMPV, as well as in disease pathogenesis. We demonstrate that signaling through IFNAR significantly contributes to increased inflammatory lung disease during HMPV infection, and therapeutics targeting this pathway may provide a way to mitigate disease symptoms. Because IFNAR signaling promotes DC expansion during early HMPV replication, elimination of this pathway results in a defect in the development of an efficient and effective CD8⁺ T cell response. These findings expand our understanding of the importance of IFNAR signaling in HMPV replication and disease, as well as suggest a mechanism for IFNAR-independent impairment of the CD8⁺ T cell response.

ACKNOWLEDGMENTS

We thank D. Flaherty, B. Matlock, and K. Weller at the Vanderbilt Flow Cytometry Shared Resource for providing technical support and assistance with the development of flow cytometry reagents. We thank M. Brissova and F. Pan at the Vanderbilt Islet Procurement and Analysis Core for providing technical support and assistance with the Aperio ImageScope slide scanner. We also thank H. W. Virgin for providing mice used in this study. A special thanks to Katherine Amato for substantial assistance in manuscript preparation and experimental design.

This study was supported by grants AI085062 (J.V.W.), AI040079 (S.J.), AI042286 (S.J.), HL054977 (S.J.), and GM007347 to the Vanderbilt Medical Scientist Training Program (J.J.E.). The Vanderbilt Medical Center Flow Cytometry Shared Resource is supported by the Vanderbilt Ingram Cancer Center (P30 CA68485) and the Vanderbilt Digestive Disease Research Center (DK058404).

REFERENCES

- Williams JV, Harris PA, Tollefson SJ, Halburnt-Rush LL, Pingsterhaus JM, Edwards KM, Wright PF, Crowe JE, Jr. 2004. Human metapneumovirus and lower respiratory tract disease in otherwise healthy infants and children. *N Engl J Med* 350:443–450. <http://dx.doi.org/10.1056/NEJMoa025472>.
- Widmer K, Zhu Y, Williams JV, Griffin MR, Edwards KM, Talbot HK. 2012. Rates of hospitalizations for respiratory syncytial virus, human metapneumovirus, and influenza virus in older adults. *J Infect Dis* 206:56–62. <http://dx.doi.org/10.1093/infdis/jis309>.
- Williams JV, Wang CK, Yang CF, Tollefson SJ, House FS, Heck JM, Chu M, Brown JB, Lintao LD, Quinto JD, Chu D, Spaete RR, Edwards KM, Wright PF, Crowe JE, Jr. 2006. The role of human metapneumovirus in upper respiratory tract infections in children: a 20-year experience. *J Infect Dis* 193:387–395. <http://dx.doi.org/10.1086/499274>.
- Williams JV, Martino R, Rabella N, Otegui M, Parody R, Heck JM, Crowe JE, Jr. 2005. A prospective study comparing human metapneumovirus with other respiratory viruses in adults with hematologic malignancies and respiratory tract infections. *J Infect Dis* 192:1061–1065. <http://dx.doi.org/10.1086/432732>.
- Englund JA, Boeckh M, Kuypers J, Nichols WG, Hackman RC, Morrow RA, Fredricks DN, Corey L. 2006. Brief communication: fatal human metapneumovirus infection in stem-cell transplant recipients. *Ann Intern Med* 144:344–349. <http://dx.doi.org/10.7326/0003-4819-144-5-200603070-00010>.
- Papenburg J, Hamelin ME, Ouhoumane N, Carbonneau J, Ouakki M, Raymond F, Robitaille L, Corbeil J, Caouette G, Frenette L, De Serres G, Boivin G. 2012. Comparison of risk factors for human metapneumovirus and respiratory syncytial virus disease severity in young children. *J Infect Dis* 206:178–189. <http://dx.doi.org/10.1093/infdis/jis333>.
- Shahda S, Carlos WG, Kiel PJ, Khan BA, Hage CA. 2011. The human metapneumovirus: a case series and review of the literature. *Transpl Infect Dis* 13:324–328. <http://dx.doi.org/10.1111/j.1399-3062.2010.00575.x>.
- Walsh EE, Peterson DR, Falsey AR. 2008. Human metapneumovirus infections in adults: another piece of the puzzle. *Arch Intern Med* 168:2489–2496. <http://dx.doi.org/10.1001/archinte.168.22.2489>.
- Edwards KM, Zhu Y, Griffin MR, Weinberg GA, Hall CB, Szilagyi PG, Staat MA, Iwane M, Prill MM, Williams JV. 2013. Burden of human metapneumovirus infection in young children. *N Engl J Med* 368:633–643. <http://dx.doi.org/10.1056/NEJMoa1204630>.
- van den Hoogen BG, de Jong JC, Groen J, Kuiken T, de Groot R, Fouchier RA, Osterhaus AD. 2001. A newly discovered human pneumovirus isolated from young children with respiratory tract disease. *Nat Med* 7:719–724. <http://dx.doi.org/10.1038/89098>.
- Dunn SR, Ryder AB, Tollefson SJ, Xu M, Saville BR, Williams JV. 2013. Seroepidemiologies of human metapneumovirus and respiratory syncytial virus in young children, determined with a new recombinant fusion protein enzyme-linked immunosorbent assay. *Clin Vaccine Immunol* 20:1654–1656. <http://dx.doi.org/10.1128/CVI.00750-12>.
- Pavlin JA, Hickey AC, Ulbrandt N, Chan YP, Endy TP, Boukhvalova MS, Chunsuttiwat S, Nisalak A, Libraty DH, Green S, Rothman AL, Ennis FA, Jarman R, Gibbons RV, Broder CC. 2008. Human metapneumovirus reinfection among children in Thailand determined by ELISA using purified soluble fusion protein. *J Infect Dis* 198:836–842. <http://dx.doi.org/10.1086/591186>.
- Okamoto M, Sugawara K, Takashita E, Muraki Y, Hongo S, Nishimura H, Matsuzaki Y. 2010. Longitudinal course of human metapneumovirus antibody titers and reinfection in healthy adults. *J Med Virol* 82:2092–2096. <http://dx.doi.org/10.1002/jmv.21920>.
- Falsey AR, Hennessey PA, Formica MA, Criddle MM, Bear JM, Walsh EE. 2010. Humoral immunity to human metapneumovirus infection in adults. *Vaccine* 28:1477–1480. <http://dx.doi.org/10.1016/j.vaccine.2009.11.063>.
- Erickson JJ, Gilchuk P, Hastings AK, Tollefson SJ, Johnson M, Downing MB, Boyd KL, Johnson JE, Kim AS, Joyce S, Williams JV. 2012. Viral acute lower respiratory infections impair CD8⁺ T cells through PD-1. *J Clin Invest* 122:2967–2982. <http://dx.doi.org/10.1172/JCI62860>.
- Schuster JE, Cox RG, Hastings AK, Boyd KL, Wadia J, Chen Z, Burton DR, Williamson RA, Williams JV. 2015. A broadly neutralizing human monoclonal antibody exhibits in vivo efficacy against both human metapneumovirus and respiratory syncytial virus. *J Infect Dis* 211:216–225. <http://dx.doi.org/10.1093/infdis/jiu307>.
- Ulbrandt ND, Ji H, Patel NK, Barnes AS, Wilson S, Kiener PA, Suzich J, McCarthy MP. 2008. Identification of antibody neutralization epitopes on the fusion protein of human metapneumovirus. *J Gen Virol* 89:3113–3118. <http://dx.doi.org/10.1099/vir.0.2008/005199-0>.
- Ren J, Kolli D, Liu T, Xu R, Garofalo RP, Casola A, Bao X. 2011. Human metapneumovirus inhibits IFN-beta signaling by downregulating Jak1 and Tyk2 cellular levels. *PLoS One* 6:e24496. <http://dx.doi.org/10.1371/journal.pone.0024496>.
- Dinwiddie DL, Harrod KS. 2008. Human metapneumovirus inhibits IFN-alpha signaling through inhibition of STAT1 phosphorylation. *Am J Respir Cell Mol Biol* 38:661–670. <http://dx.doi.org/10.1165/rcmb.2007-0285OC>.
- Barber GN. 2001. Host defense, viruses and apoptosis. *Cell Death Differ* 8:113–126. <http://dx.doi.org/10.1038/sj.cdd.4400823>.
- Sadler AJ, Williams BR. 2008. Interferon-inducible antiviral effectors. *Nat Rev Immunol* 8:559–568. <http://dx.doi.org/10.1038/nri2314>.
- Biron CA. 2001. Interferons alpha and beta as immune regulators—a new look. *Immunity* 14:661–664. [http://dx.doi.org/10.1016/S1074-7613\(01\)00154-6](http://dx.doi.org/10.1016/S1074-7613(01)00154-6).
- Havenar-Daughton C, Kolumam GA, Murali-Krishna K. 2006. Cutting edge: the direct action of type I IFN on CD4 T cells is critical for sustaining clonal expansion in response to a viral but not a bacterial infection. *J Immunol* 176:3315–3319. <http://dx.doi.org/10.4049/jimmunol.176.6.3315>.
- Le Bon A, Tough DF. 2008. Type I interferon as a stimulus for cross-priming. *Cytokine Growth Factor Rev* 19:33–40. <http://dx.doi.org/10.1016/j.cytogfr.2007.10.007>.
- Kolumam GA, Thomas S, Thompson LJ, Sprent J, Murali-Krishna K. 2005. Type I interferons act directly on CD8 T cells to allow clonal expansion and memory formation in response to viral infection. *J Exp Med* 202:637–650. <http://dx.doi.org/10.1084/jem.20050821>.
- Luft T, Pang KC, Thomas E, Hertzog P, Hart DN, Trapani J, Cebon J. 1998. Type I IFNs enhance the terminal differentiation of dendritic cells. *J Immunol* 161:1947–1953.

27. Fourcade J, Sun Z, Benallaoua M, Guillaume P, Luescher IF, Sander C, Kirkwood JM, Kuchroo V, Zarour HM. 2010. Upregulation of Tim-3 and PD-1 expression is associated with tumor antigen-specific CD8⁺ T cell dysfunction in melanoma patients. *J Exp Med* 207:2175–2186. <http://dx.doi.org/10.1084/jem.20100637>.
28. Jin HT, Anderson AC, Tan WG, West EE, Ha SJ, Araki K, Freeman GJ, Kuchroo VK, Ahmed R. 2010. Cooperation of Tim-3 and PD-1 in CD8 T-cell exhaustion during chronic viral infection. *Proc Natl Acad Sci U S A* 107:14733–14738. <http://dx.doi.org/10.1073/pnas.1009731107>.
29. Zhou Q, Munger ME, Veenstra RG, Weigel BJ, Hirashima M, Munn DH, Murphy WJ, Azuma M, Anderson AC, Kuchroo VK, Blazar BR. 2011. Coexpression of Tim-3 and PD-1 identifies a CD8⁺ T-cell exhaustion phenotype in mice with disseminated acute myelogenous leukemia. *Blood* 117:4501–4510. <http://dx.doi.org/10.1182/blood-2010-10-310425>.
30. Mühlbauer M, Fleck M, Schutz C, Weiss T, Froh M, Blank C, Scholmerich J, Hellerbrand C. 2006. PD-L1 is induced in hepatocytes by viral infection and by interferon-alpha and -gamma and mediates T cell apoptosis. *J Hepatol* 45:520–528. <http://dx.doi.org/10.1016/j.jhep.2006.05.007>.
31. McNally B, Ye F, Willette M, Flano E. 2013. Local blockade of epithelial PDL-1 in the airways enhances T cell function and viral clearance during influenza virus infection. *J Virol* 87:12916–12924. <http://dx.doi.org/10.1128/JVI.02423-13>.
32. Williams JV, Tollefson SJ, Johnson JE, Crowe JE, Jr. 2005. The cotton rat (*Sigmodon hispidus*) is a permissive small animal model of human metapneumovirus infection, pathogenesis, and protective immunity. *J Virol* 79:10944–10951. <http://dx.doi.org/10.1128/JVI.79.17.10944-10951.2005>.
33. Lissina A, Ladell K, Skowera A, Clement M, Edwards E, Seggewiss R, van den Berg HA, Gostick E, Gallagher K, Jones E, Melenhorst JJ, Godkin AJ, Peakman M, Price DA, Sewell AK, Wooldridge L. 2009. Protein kinase inhibitors substantially improve the physical detection of T-cells with peptide-MHC tetramers. *J Immunol Methods* 340:11–24. <http://dx.doi.org/10.1016/j.jim.2008.09.014>.
34. Livak KJ, Schmittgen TD. 2001. Analysis of relative gene expression data using real-time quantitative PCR and the 2(-Delta Delta C(T)) method. *Methods* 25:402–408. <http://dx.doi.org/10.1006/meth.2001.1262>.
35. Hartert TV, Wheeler AP, Sheller JR. 1999. Use of pulse oximetry to recognize severity of airflow obstruction in obstructive airway disease: correlation with pulsus paradoxus. *Chest* 115:475–481. <http://dx.doi.org/10.1378/chest.115.2.475>.
36. Rebuck AS, Pengelly LD. 1973. Development of pulsus paradoxus in the presence of airways obstruction. *N Engl J Med* 288:66–69. <http://dx.doi.org/10.1056/NEJM197301112880203>.
37. Lee SJ, Jang BC, Lee SW, Yang YI, Suh SI, Park YM, Oh S, Shin JG, Yao S, Chen L, Choi IH. 2006. Interferon regulatory factor-1 is prerequisite to the constitutive expression and IFN-gamma-induced upregulation of B7-H1 (CD274). *FEBS Lett* 580:755–762. <http://dx.doi.org/10.1016/j.febslet.2005.12.093>.
38. Eppihimer MJ, Gunn J, Freeman GJ, Greenfield EA, Chernova T, Erickson J, Leonard JP. 2002. Expression and regulation of the PD-L1 immunoinhibitory molecule on microvascular endothelial cells. *Microcirculation* 9:133–145. <http://dx.doi.org/10.1080/mic.9.2.133.145>.
39. Srivastava S, Koch MA, Pepper M, Campbell DJ. 2014. Type I interferons directly inhibit regulatory T cells to allow optimal antiviral T cell responses during acute LCMV infection. *J Exp Med* 211:961–974. <http://dx.doi.org/10.1084/jem.20131556>.
40. Golding A, Rosen A, Petri M, Akhter E, Andrade F. 2010. Interferon-alpha regulates the dynamic balance between human activated regulatory and effector T cells: implications for antiviral and autoimmune responses. *Immunology* 131:107–117. <http://dx.doi.org/10.1111/j.1365-2567.2010.03280.x>.
41. de Andrés C, Aristimuno C, de Las Heras V, Martinez-Gines ML, Bartolome M, Arroyo R, Navarro J, Gimenez-Roldan S, Fernandez-Cruz E, Sanchez-Ramon S. 2007. Interferon beta-1a therapy enhances CD4⁺ regulatory T-cell function: an ex vivo and in vitro longitudinal study in relapsing-remitting multiple sclerosis. *J Neuroimmunol* 182:204–211. <http://dx.doi.org/10.1016/j.jneuroim.2006.09.012>.
42. Namdar A, Nikbin B, Ghabaee M, Bayati A, Izad M. 2010. Effect of IFN-beta therapy on the frequency and function of CD4(+)CD25(+) regulatory T cells and Foxp3 gene expression in relapsing-remitting multiple sclerosis (RRMS): a preliminary study. *J Neuroimmunol* 218:120–124. <http://dx.doi.org/10.1016/j.jneuroim.2009.10.013>.
43. Fulton RB, Meyerholz DK, Varga SM. 2010. Foxp3⁺ CD4 regulatory T cells limit pulmonary immunopathology by modulating the CD8 T cell response during respiratory syncytial virus infection. *J Immunol* 185:2382–2392. <http://dx.doi.org/10.4049/jimmunol.1000423>.
44. Misharin AV, Morales-Nebreda L, Mutlu GM, Budinger GR, Perlman H. 2013. Flow cytometric analysis of macrophages and dendritic cell subsets in the mouse lung. *Am J Respir Cell Mol Biol* 49:503–510. <http://dx.doi.org/10.1165/rcmb.2013-0086MA>.
45. Kirby AC, Raynes JG, Kaye PM. 2006. CD11b regulates recruitment of alveolar macrophages but not pulmonary dendritic cells after pneumococcal challenge. *J Infect Dis* 193:205–213. <http://dx.doi.org/10.1086/498874>.
46. Furuhashi K, Suda T, Hasegawa H, Suzuki Y, Hashimoto D, Enomoto N, Fujisawa T, Nakamura Y, Inui N, Shibata K, Nakamura H, Chida K. 2012. Mouse lung CD103⁺ and CD11bhigh dendritic cells preferentially induce distinct CD4⁺ T-cell responses. *Am J Respir Cell Mol Biol* 46:165–172. <http://dx.doi.org/10.1165/rcmb.2011-0070OC>.
47. Seo SU, Kwon HJ, Ko HJ, Byun YH, Seong BL, Uematsu S, Akira S, Kweon MN. 2011. Type I interferon signaling regulates Ly6C(hi) monocytes and neutrophils during acute viral pneumonia in mice. *PLoS Pathog* 7:e1001304. <http://dx.doi.org/10.1371/journal.ppat.1001304>.
48. Schilte C, Couderc T, Chretien F, Sourisseau M, Gangneux N, Guivel-Benhassine F, Kraxner A, Tschopp J, Higgs S, Michault A, Arenzana-Seisdedos F, Colonna M, Peduto L, Schwartz O, Lecuit M, Albert ML. 2010. Type I IFN controls chikungunya virus via its action on nonhematopoietic cells. *J Exp Med* 207:429–442. <http://dx.doi.org/10.1084/jem.20090851>.
49. Johansson C, Wetzel JD, He J, Mikacenic C, Dermody TS, Kelsall BL. 2007. Type I interferons produced by hematopoietic cells protect mice against lethal infection by mammalian reovirus. *J Exp Med* 204:1349–1358. <http://dx.doi.org/10.1084/jem.20061587>.
50. Johnson TR, Mertz SE, Gitiban N, Hammond S, Legallo R, Durbin RK, Durbin JE. 2005. Role for innate IFNs in determining respiratory syncytial virus immunopathology. *J Immunol* 174:7234–7241. <http://dx.doi.org/10.4049/jimmunol.174.11.7234>.
51. Durbin JE, Johnson TR, Durbin RK, Mertz SE, Morotti RA, Peebles RS, Graham BS. 2002. The role of IFN in respiratory syncytial virus pathogenesis. *J Immunol* 168:2944–2952. <http://dx.doi.org/10.4049/jimmunol.168.6.2944>.
52. Gautier G, Humbert M, Deauvieu F, Scullier M, Hiscott J, Bates EE, Trinchieri G, Caux C, Garrone P. 2005. A type I interferon autocrine-paracrine loop is involved in Toll-like receptor-induced interleukin-12p70 secretion by dendritic cells. *J Exp Med* 201:1435–1446. <http://dx.doi.org/10.1084/jem.20041964>.
53. Rudd BD, Luker GD, Luker KE, Peebles RS, Lukacs NW. 2007. Type I interferon regulates respiratory virus infected dendritic cell maturation and cytokine production. *Viral Immunol* 20:531–540. <http://dx.doi.org/10.1089/vim.2007.0057>.
54. Goritzka M, Durant LR, Pereira C, Salek-Ardakani S, Openshaw PJ, Johansson C. 2014. Interferon-alpha/beta receptor signaling amplifies early proinflammatory cytokine production in the lung during respiratory syncytial virus infection. *J Virol* 88:6128–6136. <http://dx.doi.org/10.1128/JVI.00333-14>.
55. Kolli D, Bataki EL, Spetch L, Guerrero-Plata A, Jewell AM, Piedra PA, Milligan GN, Garofalo RP, Casola A. 2008. T lymphocytes contribute to antiviral immunity and pathogenesis in experimental human metapneumovirus infection. *J Virol* 82:8560–8569. <http://dx.doi.org/10.1128/JVI.00699-08>.
56. Spann KM, Loh Z, Lynch JP, Ullah A, Zhang V, Baturcam E, Werder RB, Khajornjiraphan N, Rudd P, Loo YM, Suhrbier A, Gale M, Jr, Upham JW, Phipps S. 2014. IRF-3, IRF-7, and IPS-1 promote host defense against acute human metapneumovirus infection in neonatal mice. *Am J Pathol* 184:1795–1806. <http://dx.doi.org/10.1016/j.ajpath.2014.02.026>.
57. Kadowaki N, Liu YJ. 2002. Natural type I interferon-producing cells as a link between innate and adaptive immunity. *Hum Immunol* 63:1126–1132. [http://dx.doi.org/10.1016/S0198-8859\(02\)00751-6](http://dx.doi.org/10.1016/S0198-8859(02)00751-6).
58. Ehlers M, Ravetch JV. 2007. Opposing effects of Toll-like receptor stimulation induce autoimmunity or tolerance. *Trends Immunol* 28:74–79. <http://dx.doi.org/10.1016/j.it.2006.12.006>.
59. Azuma M, Ebihara T, Oshiumi H, Matsumoto M, Seya T. 2012. Cross-priming for antitumor CTL induced by soluble Ag + polyI:C depends on the TICAM-1 pathway in mouse CD11c(+) / CD8alpha(+) dendritic cells. *Oncoimmunology* 1:581–592. <http://dx.doi.org/10.4161/onci.19893>.
60. Workman CJ, Vignali DA. 2005. Negative regulation of T cell homeostasis by lymphocyte activation gene-3 (CD223). *J Immunol* 174:688–695. <http://dx.doi.org/10.4049/jimmunol.174.2.688>.

61. Chlewicki LK, Velikovskiy CA, Balakrishnan V, Mariuzza RA, Kumar V. 2008. Molecular basis of the dual functions of 2B4 (CD244). *J Immunol* 180:8159–8167. <http://dx.doi.org/10.4049/jimmunol.180.12.8159>.
62. Sakuishi K, Jayaraman P, Behar SM, Anderson AC, Kuchroo VK. 2011. Emerging Tim-3 functions in antimicrobial and tumor immunity. *Trends Immunol* 32:345–349. <http://dx.doi.org/10.1016/j.it.2011.05.003>.
63. Nirschl CJ, Drake CG. 2013. Molecular pathways: coexpression of immune checkpoint molecules: signaling pathways and implications for cancer immunotherapy. *Clin Cancer Res* 19:4917–4924. <http://dx.doi.org/10.1158/1078-0432.CCR-12-1972>.
64. Odorizzi PM, Wherry EJ. 2012. Inhibitory receptors on lymphocytes: insights from infections. *J Immunol* 188:2957–2965. <http://dx.doi.org/10.4049/jimmunol.1100038>.
65. Kuchroo VK, Umetsu DT, DeKruyff RH, Freeman GJ. 2003. The TIM gene family: emerging roles in immunity and disease. *Nat Rev Immunol* 3:454–462. <http://dx.doi.org/10.1038/nri1111>.
66. Zhu C, Anderson AC, Schubart A, Xiong H, Imitola J, Khoury SJ, Zheng XX, Strom TB, Kuchroo VK. 2005. The Tim-3 ligand galectin-9 negatively regulates T helper type 1 immunity. *Nat Immunol* 6:1245–1252. <http://dx.doi.org/10.1038/ni1271>.
67. Santiago C, Ballesteros A, Tami C, Martinez-Munoz L, Kaplan GG, Casanovas JM. 2007. Structures of T cell immunoglobulin mucin receptors 1 and 2 reveal mechanisms for regulation of immune responses by the TIM receptor family. *Immunity* 26:299–310. <http://dx.doi.org/10.1016/j.immuni.2007.01.014>.
68. Cao E, Zang X, Ramagopal UA, Mukhopadhyaya A, Fedorov A, Fedorov E, Zencheck WD, Lary JW, Cole JL, Deng H, Xiao H, Dilorenzo TP, Allison JP, Nathenson SG, Almo SC. 2007. T cell immunoglobulin mucin-3 crystal structure reveals a galectin-9-independent ligand-binding surface. *Immunity* 26:311–321. <http://dx.doi.org/10.1016/j.immuni.2007.01.016>.
69. Sabatos CA, Chakravarti S, Cha E, Schubart A, Sanchez-Fueyo A, Zheng XX, Coyle AJ, Strom TB, Freeman GJ, Kuchroo VK. 2003. Interaction of Tim-3 and Tim-3 ligand regulates T helper type 1 responses and induction of peripheral tolerance. *Nat Immunol* 4:1102–1110. <http://dx.doi.org/10.1038/ni988>.
70. McMahan RH, Golden-Mason L, Nishimura MI, McMahon BJ, Kemper M, Allen TM, Gretch DR, Rosen HR. 2010. Tim-3 expression on PD-1+ HCV-specific human CTLs is associated with viral persistence, and its blockade restores hepatocyte-directed in vitro cytotoxicity. *J Clin Invest* 120:4546–4557. <http://dx.doi.org/10.1172/JCI43127>.
71. Golden-Mason L, Palmer BE, Kassam N, Townshend-Bulson L, Livingston S, McMahon BJ, Castelblanco N, Kuchroo V, Gretch DR, Rosen HR. 2009. Negative immune regulator Tim-3 is overexpressed on T cells in hepatitis C virus infection and its blockade rescues dysfunctional CD4⁺ and CD8⁺ T cells. *J Virol* 83:9122–9130. <http://dx.doi.org/10.1128/JVI.00639-09>.
72. Sakuishi K, Apetoh L, Sullivan JM, Blazar BR, Kuchroo VK, Anderson AC. 2010. Targeting Tim-3 and PD-1 pathways to reverse T cell exhaustion and restore anti-tumor immunity. *J Exp Med* 207:2187–2194. <http://dx.doi.org/10.1084/jem.20100643>.
73. Ngiow SF, von Scheidt B, Akiba H, Yagita H, Teng MW, Smyth MJ. 2011. Anti-TIM3 antibody promotes T cell IFN-gamma-mediated antitumor immunity and suppresses established tumors. *Cancer Res* 71:3540–3551. <http://dx.doi.org/10.1158/0008-5472.CAN-11-0096>.
74. Sehrawat S, Reddy PB, Rajasagi N, Suryawanshi A, Hirashima M, Rouse BT. 2010. Galectin-9/TIM-3 interaction regulates virus-specific primary and memory CD8 T cell response. *PLoS Pathog* 6:e1000882. <http://dx.doi.org/10.1371/journal.ppat.1000882>.
75. Kim TS, Braciale TJ. 2009. Respiratory dendritic cell subsets differ in their capacity to support the induction of virus-specific cytotoxic CD8⁺ T cell responses. *PLoS One* 4:e4204. <http://dx.doi.org/10.1371/journal.pone.0004204>.
76. Erickson JJ, Rogers MC, Hastings AK, Tollefson SJ, Williams JV. 2014. Programmed death-1 impairs secondary effector lung CD8⁺ T cells during respiratory virus reinfection. *J Immunol* 193:5108–5117. <http://dx.doi.org/10.4049/jimmunol.1302208>.
77. Alvarez R, Tripp RA. 2005. The immune response to human metapneumovirus is associated with aberrant immunity and impaired virus clearance in BALB/c mice. *J Virol* 79:5971–5978. <http://dx.doi.org/10.1128/JVI.79.10.5971-5978.2005>.
78. Melendi GA, Zavala F, Buchholz UJ, Boivin G, Collins PL, Kleeberger SR, Polack FP. 2007. Mapping and characterization of the primary and anamnestic H-2(d)-restricted cytotoxic T-lymphocyte response in mice against human metapneumovirus. *J Virol* 81:11461–11467. <http://dx.doi.org/10.1128/JVI.02423-06>.
79. Romagnani S. 2000. T-cell subsets (Th1 versus Th2). *Ann Allergy Asthma Immunol* 85:9–18; quiz 18:21. [http://dx.doi.org/10.1016/S1081-1206\(10\)62426-X](http://dx.doi.org/10.1016/S1081-1206(10)62426-X).
80. Locksley RM, Heinzel FP, Sadick MD, Holaday BJ, Gardner KD, Jr. 1987. Murine cutaneous leishmaniasis: susceptibility correlates with differential expansion of helper T-cell subsets. *Ann Inst Pasteur Immunol* 138:744–749. [http://dx.doi.org/10.1016/S0769-2625\(87\)80030-2](http://dx.doi.org/10.1016/S0769-2625(87)80030-2).
81. Gessner A, Blum H, Rollinghoff M. 1993. Differential regulation of IL-9-expression after infection with *Leishmania major* in susceptible and resistant mice. *Immunobiology* 189:419–435. [http://dx.doi.org/10.1016/S0171-2985\(11\)80414-6](http://dx.doi.org/10.1016/S0171-2985(11)80414-6).